Aalto University
School of Engineering

Kersti Haahti

Flow simulation in a ditch network of a drained peatland forest catchment in Eastern Finland

Thesis submitted in a partial fulfillment of the requirements for the degree of Master of Science in Technology.

Espoo, 18.12.2013

Supervisor: Professor Harri Koivusalo

Advisors: Professor Bassam Younis (UCDavis)
M.Sc. (Tech.) Leena Stenberg

Aalto University
School of Engineering

Aalto University, P.O. BOX 11000, 00076 AALTO
www.aalto.fi

Abstract of master's thesis

Author Kersti Haahti

Title of thesis Flow simulation in a ditch network of a drained peatland forest catchment in Eastern Finland

Department Department of Civil and Environmental Engineering

Professorship Water resources engineering **Code of professorship** Yhd-12

Thesis supervisor Professor Harri Koivusalo

Thesis advisors Professor Bassam Younis (UCDavis), M.Sc. (Tech.) Leena Stenberg

Date 18.12.2013 **Number of pages** 63 + 3 **Language** English

The suspended solid (SS) load of drained peatland forest sites after ditch network maintenance causes one of the largest strains on the water system by forestry. Understanding the hydraulic processes in newly maintained ditch networks is necessary for quantifying SS load generation and transport in source areas. In this thesis, a hydraulic unsteady flow model that would meet the needs of flow simulation in a drainage network on a forested peatland site, was built. The algorithm proposed by Zhu et al. (2011) was applied to simulate flow in a network of channels. In the iterative procedure flow in the channels of the network was solved separately using the Saint-Venant equations and the flow depths at the junction-points were corrected using the characteristic method. The algorithm was programmed using the numeric computing environment MATLAB by MathWorks. According to the hydraulic conditions produced by the model, erosion risk within the network was evaluated.

The model was applied to a newly maintained ditch network on a drained peatland catchment Koivupuro (5.2 ha) in Eastern Finland. The ditch network consisted of 15 branches, altogether 1.6 km in length, and 8 junctions. Flow simulation in the small ditches of Koivupuro with mostly very low flow rate (0.0005–0.025 m^3/s) introduced its challenges. The magnitude of flow resistance depended highly on the flow conditions. Evidently no one single Manning's coefficient could be applied for the full range of flow conditions or even for the whole network as differences in discharge were large even within the network. The variability of flow resistance introduced an inevitable challenge to flow computation over a longer time period in a network of such small scale.

The assessment of absolute erosion risk was uncertain because of the variability of flow resistance and the uncertainties related to the onsite water depth measurements. However, spatial differences in erosion risk could be derived. Based on bed shear stress evaluation the highest relative erosion risk was found in the southern end of the first and second ditch, close to the outlet of the catchment. Along these reaches flow was relatively high and the bed slope steep. In accordance with previous studies on drained peatlands, the results suggested only highest peak flows have a role in SS generation and transport in the Koivupuro ditch network.

Keywords Hydraulic modelling, ditch maintenance, peatland, erosion

Aalto-yliopisto
Insinööritieteiden korkeakoulu

Aalto-yliopisto, PL 11000, 00076 AALTO
www.aalto.fi
Diplomityön tiivistelmä

Tekijä Kersti Haahti

Työn nimi Suometsän ojaverkoston virtaamamallinnus Itä-Suomessa

Laitos Yhdyskunta- ja ympäristötekniikan laitos

Professuuri Tekninen vesitalous **Professuurikoodi** Yhd-12

Työn valvoja Professori Harri Koivusalo

Työn ohjaajat Professori Bassam Younis (UCDavis), DI Leena Stenberg

Päivämäärä 18.12.2013 **Sivumäärä** 63 + 3 **Kieli** Englanti

Metsätalouden merkittävimpänä vesistöjen kuormittajana pidetään ojitettujen soiden kiintoainekuormaa, joka on erityisen suuri kunnostusojituksen jälkeisinä vuosina. Kiintoaineen muodostumisen ja kulkeutumisen arviointi vaatii metsäojien hydraulisten prosessien ymmärrystä. Tässä työssä pyrittiin rakentamaan hydraulinen malli, joka soveltuisi metsäojaverkoston virtaaman mallinnukseen. Mallin perustana käytettiin Zhu ym. (2011) raportoimaa iteratiivista algoritmia, jossa virtaama verkoston uomissa ratkaistaan Saint-Venantin yhtälöiden avulla ja risteyskohtien vedensyvyys säädetään oikeaksi karakteristisen yhtälöiden perusteella. Mallin rakentamiseen käytettiin Mathworksin numeerista MATLAB-laskentaohjelmistoa. Mallin simuloimien virtaamaolosuhteiden perusteella pyrittiin arvioimaan eroosioriskiä uomaverkostossa.

Rakennettua virtaamamallia sovellettiin vuonna 2011 kunnostettuun ojaverkostoon Koivupurolla (5.2 ha), Sotkamossa. Ojaverkosto muodostui 15 haarasta, joiden yhteispituus oli 1.6 km, ja 8 risteyskohdasta. Virtaamamallinnus näin pienissä uomissa, joissa virtaama pysyi hyvin alhaisena (0.0005–0.025 m^3/s), oli haastavaa, sillä virtausvastus vaihteli selvästi virtausolosuhteiden mukaan. Samaa vastuskerrointa ei tämän perusteella pitäisi käyttää eri virtaamaolosuhteille saatikka koko ojaverkostolle, sillä yläjuoksulla virtaama oli huomattavasti pienempi kuin alajuoksulla. Työ osoitti, että pidemmän ajanjakson mallinnus vastaavassa ojaverkostossa on vaihtelevan virtausvastuksen takia haastavaa.

Absoluuttisen eroosioriskin määrittäminen Koivupuron ojaverkostossa oli epävarmaa, koska virtausvastuksen oletettiin vaihtelevan ja ojissa tehtyihin vedensyvyysmittauksiin liittyi epävarmuutta. Tarkastelemalla leikkausjännitystä pystyttiin kuitenkin paikantamaan verkoston eroosioalttiimmat kohdat. Suurin eroosioriski oli lähellä koealueen purkautumiskohtaa. Riskialttiit ojaosuudet kuljettivat suhteessa suurta virtaamaa ja olivat kaltevuudeltaan suuria. Kuten aiemmissa ojitetuille turvemaille kohdistuvissa tutkimuksissa, tulokset viittaavat siihen, että vain suurimmilla ylivaluntapiikeillä on kiintoainekuormituksen kannalta merkittävä rooli.

Avainsanat Hydraulinen mallinnus, kunnostusojitus, turvemaa, eroosio

Acknowledgements

I would like to thank Professor Harri Koivusalo for offering me an interesting subject for my Master's thesis and for the exceptional opportunity to carry out part of the work in UCDavis, California. I am very grateful for the Aalto University School of Engineering for providing the funding for my work and travel arrangements. Also the Finnish Forest Research Institute (METLA) is acknowledged for providing the data.

I further want to thank my supervisor Professor Harri Koivusalo for all his support and interesting conversations. I would also like to thank my advisor Leena Stenberg for processing the data from the study site and her continuous readiness to answer all my questions about the data and the study site.

This Master's thesis was made in cooperation with the University of California in Davis where I spent two months working on the computational part of my thesis. I want to thank Professor Bassam Younis who was my advisor at UCDavis for all the arrangements, his encouragement and the comments he gave about my work.

I am thankful for the whole Water Engineering research group for the pleasant working environment and the nice company. Lastly, I want to thank my family and friends for the support they have given me, especially my partner Lauri who has supported me throughout the process and provided me the most welcome traveling companion to Davis, California.

Espoo, 18.12.2013

Kersti Haahti

Table of contents

Notation

A = cross-sectional area of flow [m^2]
c = kinematic wave celerity [m/s]
ET = evapotranspiration [mm/d]
Fr = Froude number [-]
H = height of cross-section [m]
h = flow depth [m]
h_b = flow depth at junction-point [m]
h_{weir} = distance from the ditch bottom to the bottom of the V-notch weir [m]
I_m = incidence matrix [-]
L_1 = bottom width of cross-section [m]
L_2 = top width of cross-section[m]
O_{drain} = runoff to the stream network [mm/d]
P = wetted perimeter [m]
Pr = precipitation [mm/d]
Q = discharge [m^3/s]
R = hydraulic radius [m]
Re = Reynolds number [-]
S_0 = bottom slope [-]
S_f = friction slope [-]
ΔS = change in storage [mm/d]
T = spread [m]
g = acceleration due to gravity [m/s^2]
M = total number of channels in network [-]
N = total number of nodes in channel [-]
n = Manning's roughness coefficient [-]
q = lateral inflow per unit length [m^2/s]
r = radius characterizing side arc of cross-section [m]
T_r = hydrograph's time of rise [s]
t = time [s]
t_{lag} = time lag of flood wave [s]
Δt = time step of flow simulation [s]
v = velocity [m/s]
v_k = kinematic viscosity [m^2/s]
x = longitudinal distance [m]
Δx = longitudinal distance step of flow simulation [m]
α = time weighting coefficient of Preissmann scheme [-]
τ_b = bed shear stress [N/m^2]
τ_{cr} = critical shear stress [N/m^2]
ρ = density of water [kg/m^3]

Subscripts

i = index for computational node

I	=	index for iteration round in Newton-Raphson algorithm
in	=	index for incoming channels
K	=	index for iteration round in junction-point prediction correction algorithm
out	=	index for outgoing channels

Superscripts

k	=	index for time step

Abbreviations

DBH	Diameter at breast height
LAI	Leaf area index
LS	Woody sphagnum peat
LSC	Woody sphagnum-carex peat
SS	Suspended solids

List of figures

List of tables

1 Introduction

One third the land area in Finland is covered by peatlands (Finnish Statistical Yearbook of Forestry 2012). Today 4.5 million ha of peatland are drained for forestry purposes, which is about half of the total land area of peatlands in the country (Peltomaa 2007). The objective of the drainage of peatlands is to lower the high water table in peatlands and create better circumstances for tree growth. The most active period of forest drainage was in 1960–1970 (Joensuu et al. 1999). Since the 1990s ditching is no longer conducted on peatlands and the focus has switched to the maintenance of existing ditch networks (Peltomaa 2007). It has been estimated that one third of the drained peatlands in Finland are in need of ditch network maintenance (Koivusalo et al. 2008a).

In time after the initial drainage the condition of the ditches, or their drainage capacity, deteriorates which might weaken the circumstances for three growth (Päivänen 2007). In order to sustain forest productivity ditch networks are maintained, i.e. ditches are cleaned or supplementary ditching is conducted. Typically ditch network maintenance is conducted every 20–40 years to improve drainage capacity of the ditches (Lappalainen et al. 2010). Nevertheless, not all sites with ditches in visually poor condition necessarily require ditch network maintenance since interception and transpiration by a mature and vigorously growing tree stand can maintain sufficiently low water level for undisturbed tree growth (Sarkkola et al. 2010; Sarkkola et al. 2012). Since ditch network maintenance is a notable operational cost and deteriorates water quality in receiving rivers and lakes unnecessary maintenance operations should be avoided (Hökkä et al. 2008).

Flow on the bare soil of the cleaned ditches enables erosion and the transport of suspended solids (SS) into the receiving rivers and lakes. According to Joensuu et al. (1999) the SS load from a drained peatland increases remarkably after maintenance operations. Especially during the first year after maintenance the SS load remains high. On peatlands the discharge in the relatively closely dug feeder ditches (spacing 30–50 m) is usually small, which mainly rules out erosion in normal conditions. On the other hand collecting ditches conduct considerably larger amounts of water and have a higher risk of erosion (Joensuu et al. 1999). The SS load depends on the discharge: Marttila and Kløve (2010) report that the majority of the SS load is generated during summer peak discharges and spring season snowmelt.

The SS load after ditch network maintenance on peatlands causes one of the largest strains on the water system by forestry (Koivusalo et al. 2008b). Therefore it is important to understand the hydraulic processes in newly maintained ditches and be able to estimate the erosion rate and the transport of SS within the ditch network. The ability to predict the SS load and its spatial distribution would help in the assessment of land use impacts such as drainage and in the design of water protection methods (Marttila and Kløve 2010). Knowledge can contribute to practical water protection work, for example Marttila and Kløve (2008) determined a critical value of 0.15 m/s for flow velocity above which a peat layer will be eroded. Then again Lappalainen et al. (2010) modeled

sediment transport in a single ditch on a forested peatland and concluded that the main factors controlling erosion and sedimentation were the particle size, the bed roughness height, Manning's roughness coefficient, the bed slope and discharge.

Assessment of the spatial distribution of sediment processes in a watercourse is coupled with hydraulic modeling of the watercourse (e.g. Lappalainen et al. 2010). Usually the Saint-Venant equations are used to simulate unsteady flow in open channels (French 1986). Flow modeling in a single channel is relatively simple (Islam et al. 2005). Szymkiewicz (2010) outlines a frequently used solution algorithm that is based on the numerical solution of the Saint-Venant equations using the four-point implicit Preissmann scheme and the Newton-Raphson iterative method. In order to solve the Saint-Venant equations an initial condition and boundary conditions both up- and downstream are required in a single channel (Cunge et al. 1980). The iteration process of implicit flow simulation in a single channel with N computational nodes requires the simultaneous solution of $2N \times 2N$ linear equations (French 1986). The coefficient matrix of this system of linear equations is banded, which enables efficient matrix solution algorithms and reduces the required storage from $4N^2$ to a maximum of $8N$ (Fread 1973a).

In a more general case the watercourse is not usually formed only by a single channel but a network of channels. Compared to a single channel, flow routing in a network is more complicated because of the presence of backwater effects at channel junctions which prevent us from simulating flow independently in the channels of the network (Islam et al. 2005). Numerous researches have investigated simulation of unsteady flow in channel networks. Typically the simultaneous solution of the entire network requires large computer memory and lacks efficiency (Islam et al. 2005). Compared to flow routing in a single channel, the coefficient matrix is now much larger, $2\sum N_m \times 2\sum N_m$ where m refers to the index of the branch (Szymkiewicz 2010). Additionally the matrix is not banded anymore preventing efficient solution and requiring more storage space. A great deal of algorithms have been developed to reduce computational difficulty. The earliest ones assumed tributary flow as lateral inflow to the main channel simplifying the problem back to a single channel problem (e.g. Fread 1973a). Later multiple studies considered specific node-numbering schemes to reduce the bandwidth of the solution matrix (e.g. Nguyen and Kawano 1995; Naidu et al. 1997). However, in a general network of channels it is difficult to use a specific node numbering scheme (Zhu et al. 2011). Further development led to new algorithms which no longer required any specific node-numbering scheme (e.g. Sen and Garg 2002; Zhu et al. 2011).

Sen and Garg (2002) presented an iterative algorithm for solving flow in a channel network that consists of separating the end-node variables of all branches and solving them from a global matrix and then using the end-node variables to solve flow in each branch of the network independently. This reduces the size of the coefficient matrix to $4M \times 4M$, where M is the number of branches in the network. While this is much less than the dimensions of the matrix for the entire network, it can still be very time consuming if M is large (Zhu et al. 2011). To avoid solving a large global matrix a novel method was proposed by Zhu et al. (2011). The method treats backwater effects at junc-

tion-points by means of flow depth prediction and correction. Similarly to the method of Sen and Garg (2002) the flow in the channels is simulated independently. Compared to each other the algorithm of Zhu et al. (2011) shows better efficiency in storage requirements, ca. 30 % faster computation time and is easy to program (Zhu et al. 2011). The advantage of the algorithm of Zhu et al. (2011) increases with the ratio of the number of branches to the total number of nodes in the network.

Flow simulation requires the estimation of flow resistance (French 1986). Modeling flow in small channels is highly subject to errors because singular roughness elements, such as individual logs, roots or rocks, may contribute to significant energy losses when the flow depth is small (Järvelä and Helmiö 2004). Because of the variations of discharge in small streams, different resistance coefficients should be used for flows of different magnitude (Niemi 2010). A constant Manning's resistance coefficient for low to high flows will result in incorrect results, which introduces us the difficulties of unsteady flow simulation across a full range of flow conditions in small streams. It is expected that Manning's coefficient is dependent on the turbulence of the flow (French 1986). Hosia (1980) reported a relationship between Reynolds number and Manning's resistance coefficient in small scale Finnish streams. According to the study Manning's coefficient can increase remarkably when Reynolds number decreases.

The primary aim of this study was to build a hydraulic model for unsteady flow in a channel network and apply the model to the maintained ditch network of a small peatland forestry catchment Koivupuro in Eastern Finland. According to the modeling results we tried to gain better understanding of the hydraulic conditions in peatland drainage ditches and of problems relied to flow simulation in small streams. The flow simulation model would function as a basis for evaluating transportation of suspended solids in the maintained ditch network. In the scope of this work the relative erosion risk along the ditches of the drainage network was analyzed but no attention was given to the actual load of suspended solids. A secondary point of interest was the time lags in the hydrological and hydraulic processes. The study aimed to identify how big the role of the hydraulic processes in the network had compared to the time lag from a precipitation event to the discharge peak at the outlet of the catchment.

2 Background

2.1 Hydrology of a forested catchment

Water enters and leaves a forested catchment area through different processes and forms (Koivusalo et al. 2007). The water balance of a forested catchment can be considered in two domains: the forested catchment is composed of land areas outside the stream network and the stream network itself (Koivusalo et al. 2009). On the forested land areas of the catchment the water balance components consist of precipitation in the form of water or snow, runoff to the stream network, evapotranspiration and the storage of water (Equation (1)).

$$Pr = O_{drain} + ET + \Delta S \tag{1}$$

where Pr [mm/d] is precipitation, O_{drain} [mm/d] is runoff to the stream network, ET [mm/d] is evapotranspiration and ΔS [mm/d] is the change in storage.

On the forested land areas part of the precipitation is intercepted by the foliage of the stand and the understory vegetation. Evaporation from the surface of leaves of the vegetation is called interception. Evapotranspiration consists of evaporation from the ground and interception and transpiration by the vegetation. Runoff can be conceptualized as surface or groundwater runoff. Surface runoff may occur during high precipitation events when the soil profile becomes fully saturated. Figure 1 represents the components of the water balance of a forested land area.

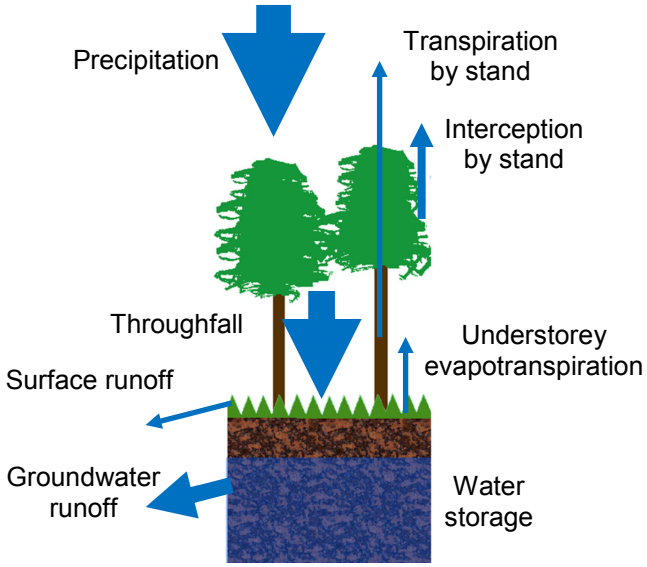

Figure 1 *Water balance components of a forested catchment.*

The stream network, the second water balance domain of the catchment, receives the runoff from the land areas of the catchment (O_{drain}; Koivusalo et al. 2009). The runoff from the land areas can be applied as the input for flow routing in the stream network. Furthermore, there is some water entering the open streams directly in the form of precipitation and on the other hand water evaporating from the free water surface of the

stream. Because of the short time lag of the stream network precipitation to the stream network and evaporation from the stream network are usually neglected (e.g. Koivusalo et al. 2006). The flow exiting the stream network at the outlet represents the runoff of the whole forested catchment.

2.2 Open channel hydraulics

2.2.1 Basic concepts

In an open channel part of the flowing stream is exposed to the atmosphere (Szymkiewicz 2010). An open channel can be either prismatic or non-prismatic. In a prismatic channel the cross-sectional shape and the longitudinal bottom slope are constant along the length of the channel (Szymkiewicz 2010). The characteristics of prismatic channels can obviously only be possessed by artificial channels. Non-prismatic channels on the contrary have varying cross-sectional area and bottom slope along the channel. In the view of computational hydraulics important cross-sectional elements are flow depth h [m], flow area A [m^2], top width or spread T [m], wetted perimeter P [m] and hydraulic radius R [m] which is the flow area divided by the wetted perimeter (French 1986; Figure 2).

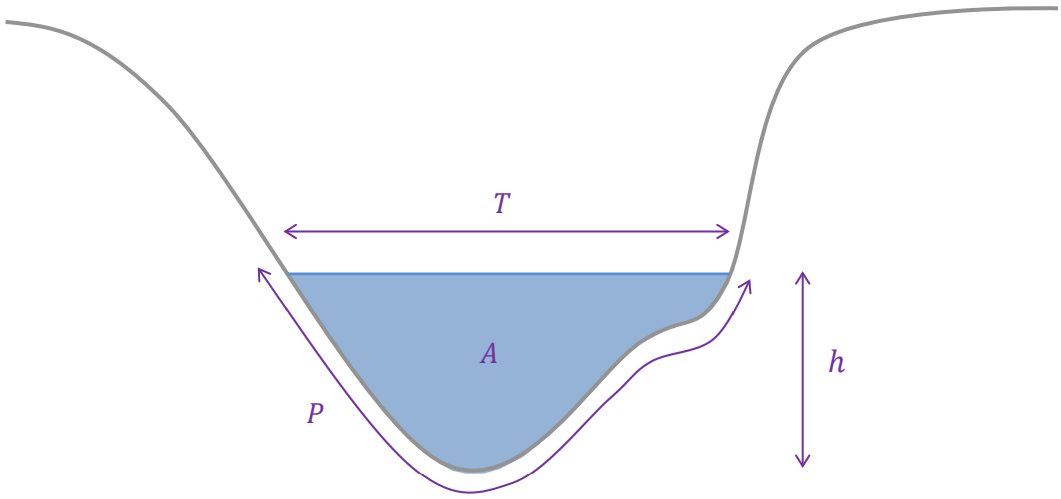

Figure 2 *Cross-sectional elements of an open channel.*

Flow in open channels can be classified in many ways (Szymkiewicz 2010). One of the primary criteria of classification is the variation of flow depth in time and space (French 1986). If flow depth remains constant in time the flow is referred to as steady. On the other hand, flow is called unsteady if it changes with time. For example during a flooding event the flow and water depth in the channel vary with time making the flow unsteady. Another way to classify flow is to define it as one- or multi-dimensional, which is important from the point of view of flow simulation. In one-dimensional flow the velocity is assumed to be uniform over the cross-section and the water level across the cross-section is horizontal (Cunge et al. 1980).

Flow can be classified as subcritical, critical and supercritical flow using a parameter called Froude number (Fr; French 1986). Subcritical flow ($Fr < 1$) is the typical form of flow in channels and is characterized by relatively high flow depths and low velocities.

Supercritical flow ($Fr > 1$) on the other hand has typically low flow depth and high velocities (Szymkiewicz 2010). An important difference between subcritical and supercritical flow is that in subcritical flow disturbances travel both in upstream and downstream directions, but in supercritical flow disturbances travel only in downstream direction (French 1986).

The distinction between laminar and turbulent flow depends on the ratio of inertial forces to viscous forces (French 1986). In laminar flow the water particles appear to move in definite, smooth paths which do not intersect. In turbulent flow the viscous forces are weak compared to inertial forces causing water particles to move in chaotic, irregular paths which intersect. Flow is called transitional between laminar and turbulent flow. The basis for this classification is the Reynolds number:

$$Re = \frac{vR}{v_k} \tag{2}$$

where v [m/s] is the flow velocity, v_k [m^2/s] is the kinematic viscosity of water and R [m] is the hydraulic radius. Open channel flow is laminar if $Re < 500$, transitional if $500 \leq Re \leq 12\,500$ and turbulent if $Re > 12\,500$ (French 1986).

Natural channels, like rivers or streams, often have tributaries or they diverge into multiple channels forming channel networks. Channel networks which only have converging channel junctions are called dendritic or tree-like networks (Kujita 1995). The other class of networks is formed by the looped networks in which channel junctions can be both diverging and converging. Figure 3 illustrates the difference between dendritic and looped channel networks.

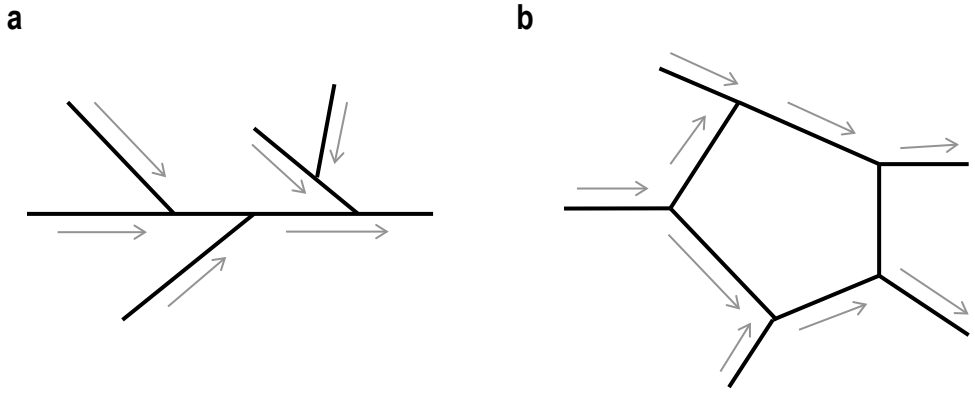

Figure 3 *Example of a dendritic (a) and a looped channel network (b).*

2.2.2 Flow resistance

Any open channel has an ability to resist flow. Flow resistance can be contributed by bed roughness, separation of flow over small-scale structures and resistance associated with large-scale bed unevenness (Järvelä and Helmiö 2004). In practical engineering the Manning's coefficient is the most widely used coefficient that attempts to quantify this property. The larger the Manning's coefficient is the higher the resistance of flow. It is

well known that estimating an appropriate value of resistance is very difficult in practice because it is expected that flow resistance depends among others on the channel cross-section, flow depth, discharge and vegetation (Hosia 1980; French 1986).

The most common and simplest way to estimate a value for Manning's coefficient is to use the values from literature (Järvelä 1998). Several sources list photographs and verbal descriptions of different channel types and Manning's coefficient corresponding to the described environments. Probably the most applied selection of pictures and descriptions is documented by Chow (1959). However, the values presented in literature are usually obtained for mean or high flow situations and often for bigger channels than common drainage ditches and channels (Hosia 1980; Niemi 2010). For smaller scale streams in Finland Saari (1955) has documented tables and pictures and the corresponding Manning's coefficients.

2.2.3 Governing equations of 1D unsteady flow

One-dimensional unsteady flow in open channels is described by the Saint-Venant equations which are based on the conservation of mass and momentum (Cunge et al. 1980). The Saint-Venant equations are expressed as follows

$$\frac{\partial A}{\partial t} + \frac{\partial Q}{\partial x} - q = 0 \tag{3}$$

$$\frac{\partial Q}{\partial t} + \frac{\partial}{\partial x}\left(\frac{Q^2}{A}\right) + gA\frac{\partial h}{\partial t} + gA(S_f - S_0) = 0 \tag{4}$$

where A [m^2] is the cross-sectional flow area, Q [m^3/s] is the discharge, q [m^2/s] is the lateral inflow per unit length, h [m] is the flow depth, g [m/s^2] is the acceleration due to gravity, S_f is the friction slope, S_0 is the bottom slope, x [m] is the longitudinal distance along channel and t [s] is time. The friction slope in the momentum equation (Equation (4)) can be estimated by the Manning's flow resistance equation

$$S_f = \frac{n^2 Q|Q|}{A^2 R^{4/3}} \tag{5}$$

where n is Manning's coefficient and R [m] is the hydraulic radius. The derivation of the above equations includes multiple assumptions (Cunge et al. 1980; Szymkiewicz 2010). It is assumed that the channel bottom slope is small, the lateral inflow does not influence the momentum balance, the friction slope is estimated as for steady flow and the streamline curvature is small.

The Saint-Venant equations may be applied to long reaches of natural rivers or channels but only seldom to the entire length of a modeled watercourse (Cunge et al. 1980). In channel networks discontinuities are formed by channel junctions and separate equations need to be applied for the junction-points to link the channels to each other. The so called inner boundary conditions are derived from the conservation of mass and energy

(Cunge et al. 1980). The conditions state that the sum of the discharges at the junction is zero (Equation (6)) and that the flow depths at the junction are equal (Equation (7)).

$$\sum Q = \sum Q_{in} - \sum Q_{out} = 0 \tag{6}$$

$$h_{in} = h_{out} \tag{7}$$

where subscript *in* refers to the incoming channels and *out* to the outgoing channels.

2.3 Erosion and sediment transport

Driving forces of erosion are mainly water, wind and ice. Erosion in a catchment can occur on the ground surface as sheet erosion due to rain and surface runoff or in the open channels of the catchment as channel erosion (Seuna and Vehviläinen 1986). On drained forest catchments sheet erosion can be expected to be low compared to channel erosion, especially after maintenance of the ditches (Lappalainen 2008; Tuukkanen 2010). However, cleaning of ditches is often conducted simultaneously with tree cutting during which the understorey vegetation gets damaged by machinery and the land is subject to tilling (Koivusalo et al. 2008b). Runoff on the bare soil after tree cuttings may trigger sheet erosion on the land areas.

Flow in open channels has the ability to scour channel beds, to carry sediment particles and deposit materials (Chanson 1999). The transport of sediment by flow in open channels can be in the form of bed-load or suspended load (van Rijn 1984). The distinction between bed and suspended load is somewhat arbitrary. Usually the bed-load transport is defined as the transport of particles by rolling, sliding and saltating along the bed surface and suspended load refers to the particles maintained in suspension by turbulence (van Rijn 1984; Chanson 1999; Figure 4). The transport mechanism of sediment depends primarily on flow conditions and the properties of the sediment (Tuukkanen 2010).

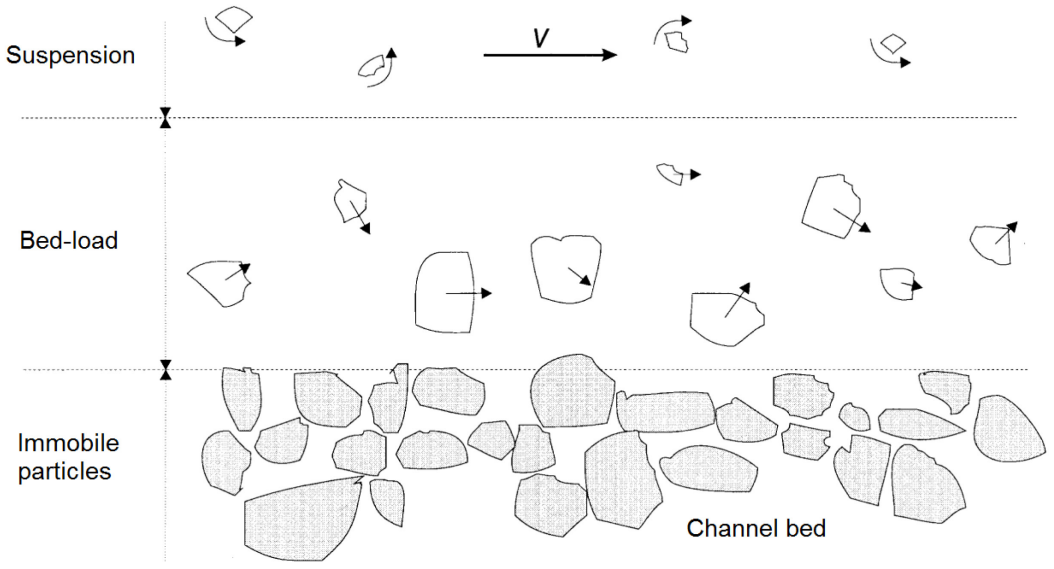

Figure 4 *Sketch of forms of sediment transport in an open channel (Chanson 1999, modified).*

Particle detachment from the bed occurs when a critical state is reached (Graf 1984). Although the detachment of particles occurs randomly the critical state is characterized using a critical velocity or more commonly a critical bed shear stress (Vanoni 1984). When the bed shear stress exceeds a critical value, the particles will start rolling and sliding in continuous contact with the bed (van Rijn 1984). The parameter associated with particles moving into suspension is the fall velocity of the particle (Vanoni 1984). When the value of flow velocity close to the bed exceeds the fall velocity of the particles, the sediment particles can be lifted to a level where the upward turbulent forces may transfer the particles into suspension (van Rijn 1984).

The erosion rate of particles depends on their size and the force holding them in place on the channel bed is gravity. However, with finer sediments cohesive forces are more dominant than the gravity of a single particle (Grag 1984). Because of dominating cohesive forces it is not possible to predict the critical shear stress for bed erosion solely on particle size or other easily measurable parameters (Marttila and Kløve 2008). Also the transport of cohesive sediments is different compared to coarser sediment because they travel as aggregated groups of particles rather than separately (McAnally and Mehta 2000).

The total sediment load can be obtained either by addition of separately computed bedload and suspended load or by directly calculating the total load (Graf 1984). Equations for total load are usually established empirically and therefore the parameters in the equations are bound to certain conditions and should be applied with caution in new sites and conditions (Graf 1984; Vanoni 1984). A relation between total erosion rate and excess shear stress can for example be obtained empirically and even be applied for cohesive bed material (e.g. Parchure and Mehta 1985; Marttila and Kløve 2008).

3 Koivupuro catchment area

3.1 Site description

The study site was a 1.13 km^2 drained peatland catchment Koivupuro situated in Eastern Finland (63°53' N, 28°40' E; Figure 5). The mean annual temperature during 1981–2010 in the area was 2.3 °C and the mean annual precipitation 591 mm (Finnish Meteorological Institute 2012). The Koivupuro catchment was initially drained by an open ditch network in 1983 for forestry purposes and has been monitored since 1978. During the following decades several clear cuttings have been performed in parts of the catchment. In 2011 a research project was started to study the erosion processes after maintenance of ditches. Thus in August 2011 part of the Koivupuro catchment ditch network was maintained creating simultaneously a smaller nested catchment in the area for intensive monitoring (Figure 6). The ditches at the edges of the nested catchment were blocked to avoid inflow from the surrounding areas and to ensure that water would flow out only at the southern end outlet of the nested catchment.

Figure 5 *Location of the Koivupuro catchment in Eastern Finland.*

The main focus of this study was on the small nested catchment in the Koivupuro area. The experimental area was 5.2 ha in size and the total length of the cleaned ditch network was 1.6 km. The ditch spacing was ca. 35 m. The ditches left unmaintained in the nested catchment in August 2011 (ca. 0.1 km; Figure 6) had grown partly shut and were less deep than the maintained ditches (Figure 7). As a result the remaining unmaintained ditches had a minor role in conducting water out of the area.

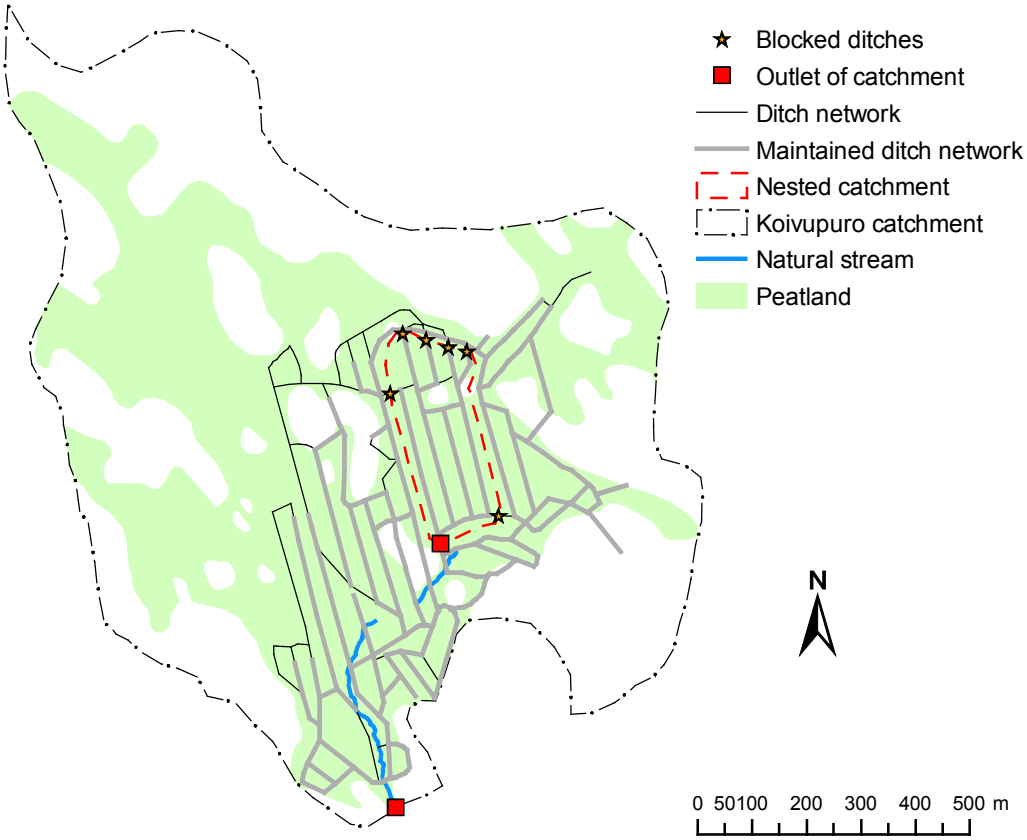

Figure 6 *Koivupuro catchment and the smaller nested catchment formed after ditch network maintenance in August 2011.*

Figure 7 *Example of maintained (a) and unmaintained (b) ditch in the Koivupuro nested catchment in Eastern Finland. (Pictures Kersti Haahti)*

The soil type of the experimental area was mostly peat (Figure 6). The depth of the peat layer varied from 0 m up to 4 m. Mostly the peat was either woody sphagnum peat (LS)

or woody sphagnum-carex peat (LSC). The decomposition of the peat in the area was on the Von Post scale 3–8. The majority of the ditches of the nested catchment were peat down to the ditch bottom, only a minority reached the sandy mineral soil (ditches around white area in Figure 6).

The study area was slight sloping (mean slope 1 %), the highest areas being in the northern part and the lowest in the southeastern part of the catchment (Figure 8). The area was covered by a Scots pine (*Pinus sylvestris*) dominated stand with a mixture of Norway spruce (*Picea abies*) and Birch (*Betula pendula*). The stand volume was 89 m^3/ha in 2012. The understorey consisted mainly of springs of bilberries, sedge and sphagnum moss.

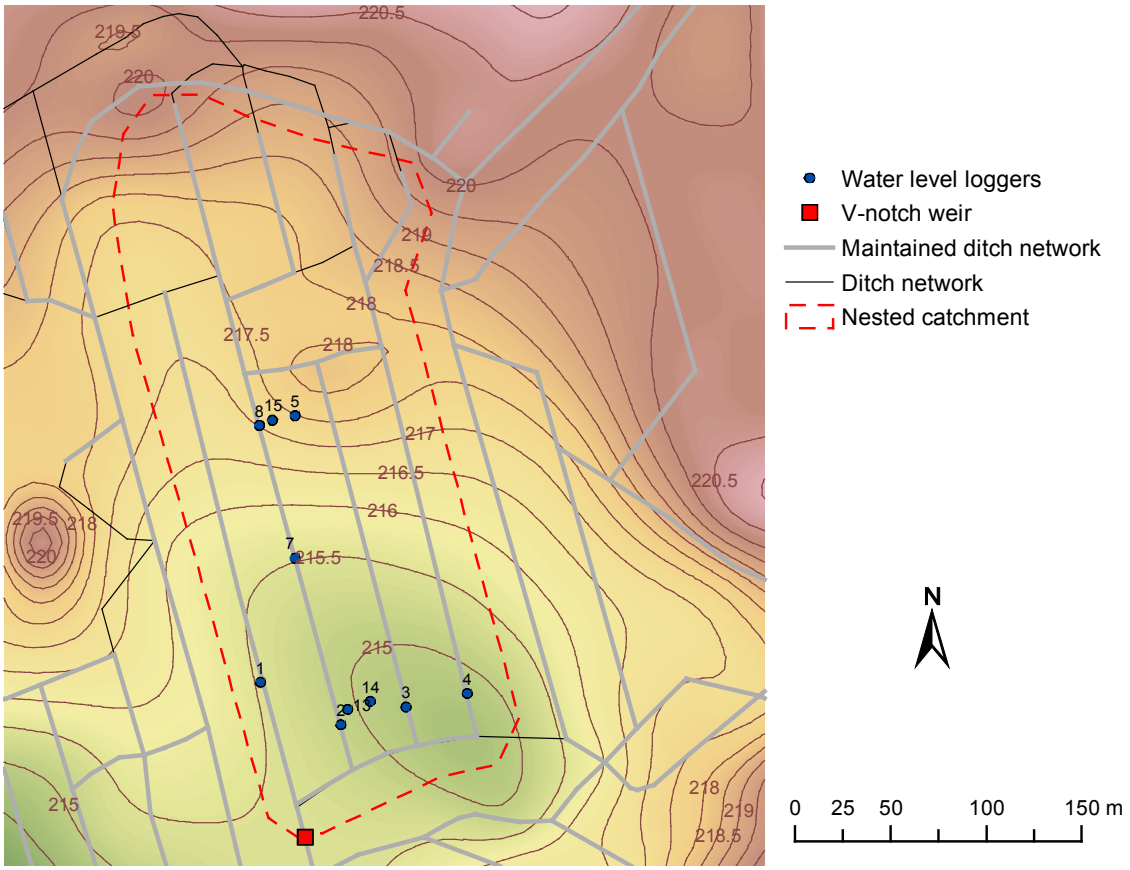

Figure 8 *Elevation (m) and location of water level measurement loggers and the V-notch weir for discharge measurements in the small nested catchment of Koivupuro.*

3.2 Measurements

Meteorological data were provided from a weather station of METLA (Finnish Forest Research Institute) called Iso-Kauhea located 3 km away from the Koivupuro catchment. The data included air temperature, precipitation, wind speed, relative humidity, global radiation and sunshine moments recorded at a 20 minute interval.

The number of stems, diameter at breast height (DBH) and stand height were determined using systematically selected experimental plots inside the studied nested catchment. Each characteristic was determined separately for Scots pine, Norway spruce and Birch.

In the nested catchment of Koivupuro water level in the ditches was measured at 6 locations and ground water table at 4 locations (Figure 8) with automatic Trutrack WT-HR Water Height loggers (Figure 9a). Measurements were taken at a resolution of 1 mm every 15 minutes during the frost free period since August 2011. In 2012 the loggers 5 and 8 were malfunctioning. The loggers were 20 mm diameter stainless steel tubes with measuring ranges of 1.5 m, 1 m or 0.25 m. The loggers were placed in perforated pipes installed in the bottom of the ditch or in the ground. The stage of the bottom of the loggers was leveled in 2011 and 2013. The accuracy of the Trutrack loggers was ± 1 % of the measuring range. The measured flow depths varied in the range of 0.05–0.30 m.

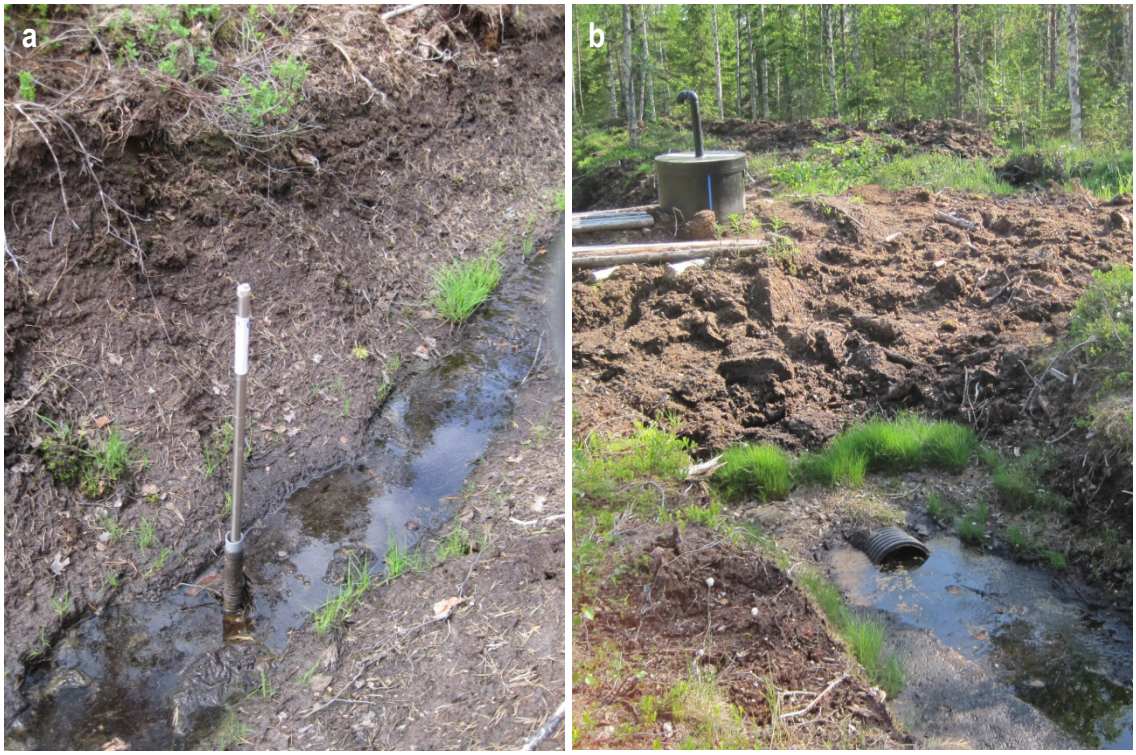

Figure 9 *Trutrack logger for water level measurements in a ditch (a) and the measurement well at the outlet of the Koivupuro nested catchment (b). (Pictures Kersti Haahti)*

Discharge was measured at the outlet of the nested catchment (Figure 8) using a V-notch weir of 90° and a pressure sensor. Water stage was measured by the pressure sensor every 15 minutes during the unfrozen period. The discharge was produced using the known stage-discharge relationship:

$$Q = 1.381h^{5/2} \tag{8}$$

where Q [m^3/s] is discharge and h [m] is water depth from the bottom of the V-notch weir. The distance between the bottom of the V-notch and the bottom of the ditch was about 0.27 m. The well where the weir and the pressure sensor were installed is shown in Figure 9b. In the summer months of 2012 several flow events were recorded, the highest momentary discharge reaching 0.025 m^3/s (Figure 10). As shown by the discharge time series a base flow of ca. 0.001 m^3/s remains at the catchment outlet even during longer dry periods.

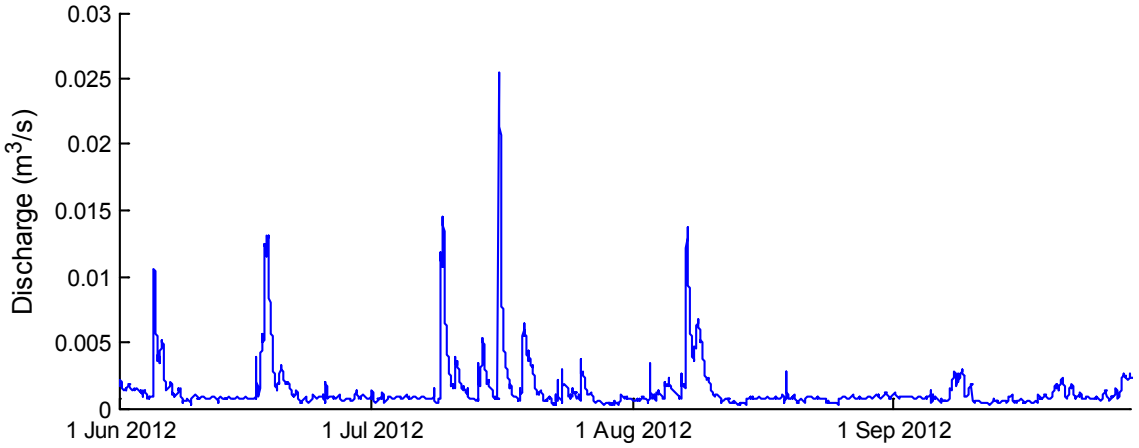

Figure 10 *Measured discharge at the outlet of the nested catchment of the Koivupuro area in June–September 2012.*

The bottom elevation of all the cleaned ditches of the nested catchment was leveled every 10 meters in September 2011 at an accuracy of 0.01 m. Furthermore, a 10×10 m^2 grid elevation data (National land survey of Finland) were available for the catchment area.

4 Methods

4.1 Inflow to ditches

4.1.1 Flow accumulation

In the Koivupuro ditch network flow enters the channels in the form of lateral inflow along all the channels. It is assumed that there is no flow entering the smaller catchment from outside but that all the flow in the ditches is originated from precipitation in the catchment area. Flow direction and flow accumulation in the catchment were determined on the basis of the elevation raster using the geospatial processing program ArcMap. The flow accumulation area was calculated at a 1 m interval for each channel of the network.

First, an idealized channel network (average slope 0.01) was sunk into the interpolated 1×1 m^2 grid elevation raster. Flow direction was produced using the single-direction flow algorithm D8 (Jenson and Dominique 1988) which gives each cell a value that represents the direction of the steepest drop (eight possible directions). Cells that are lower than all of their neighboring cells are called sinks and needed to be filled before proceeding to the next step. Filling a sink is comparable to the sink being full of water.

Flow accumulation was then computed resulting in a raster with values presenting the amount of cells from which the flow accumulates to the current cell. As the cell size was 1 m^2 the raster values corresponded directly to the flow accumulation area of each cell. Flow accumulation values along the channels were extracted from the raster at a 1 m interval. The flow accumulation area corresponding to the lateral inflow at each node in the ditch was calculated by subtracting flow accumulation of the upstream node(s) from flow accumulation of the current node.

The flow accumulation area of lateral inflow of each node in the ditch was divided by the total number of cells, resulting in values that represented fractions of the catchment runoff. For example, if the value of a certain node in the ditch was 0.1, it would mean 10 % of the catchment runoff entered the ditch at this point.

4.1.2 Modeling catchment runoff

The hydraulic model constructed in this thesis will primarily be using the measured discharge at the outlet of the catchment as the input of the model. The input discharge will be distributed as incoming lateral inflow along the ditches according to the inflow coefficients (see previous section 4.1.1). As an alternative to the measured discharge at the outlet of the ditch network an estimate of runoff was produced by a hydrological model FEMMA (Koivusalo et al. 2006; Koivusalo et al. 2008a; Koivusalo et al. 2009). The model reads meteorological data as input and calculates water balance components. The model simulates interception and transpiration of over- and understorey vegetation, soil and groundwater movement, and runoff generation. Additionally, in winter time the model would account for snow accumulation and melt, which in the case of our study was of no interest.

The input meteorological data consists of hourly continuous time series of air temperature, precipitation, wind speed, relative humidity, global radiation and long-wave radiation. Apart from long-wave radiation all the variables were measured at Iso-Kauhea. Long-wave radiation was estimated based on the measurements of air temperature, relative humidity and sunshine hours following the method described by Turunen (2011). The canopy model included in FEMMA simulates the meteorological variables beneath the forest canopy, except for relative humidity and air temperature which are assumed not to be affected by the canopy. The potential evapotranspiration is calculated in the model for the under- and overstorey using the Penman-Monteith equation. The potential evapotranspiration is primarily used for evaporation of the intercepted water. When all intercepted water is depleted, i.e. the canopy is dry, transpiration starts to occur.

The required parameters characterizing vegetation are the mean stand height, the mean DBH, the leaf area index (LAI) and canopy density for both under- and overstorey. The understorey canopy density was set to the value of 1 (i.e. 100 % coverage). For the overstorey LAI and the canopy density of the stand were estimated based on the stand measurements. First the needle biomasses corresponding to Scots pine, Norway spruce and Birch of average proportion were estimated applying the simple biomass functions of Repola et al. (2008). The biomasses for the three different tree species were then multiplied with their stem number in the study site and their specific needle area (estimates from Kellomäki 1999) to produce an estimate of leaf area for each species. The overall LAI was then calculated by dividing the sum of leaf area by the area of the study site, resulting in 1.6 m^2/m^2. The method proposed by Pomeroy et al. (2002) was applied to derive canopy density directly from the LAI estimate. The estimate for canopy density of the overstorey was 0.7.

The soil water movement and runoff generation is modeled by FEMMA in a typical longitudinal section from a water divide to an open channel, e.g. a ditch. This profile is divided into vertical soil columns and further into horizontal soil layers. The model computes first the vertical fluxes in the unsaturated zone of the soil columns based on the Richard's equation. Water that cannot infiltrate is transported downslope as surface runoff until it either reaches the ditch or infiltrates into the soil further down the profile. Based on the resulting groundwater levels in the soil columns the lateral groundwater flow between the soil columns is computed according to Darcy's law. As a boundary condition the groundwater flow model needs the water level in the ditch. Figure 11 illustrates the quasi-two-dimensional modeling of water fluxes in the soil by the FEMMA model.

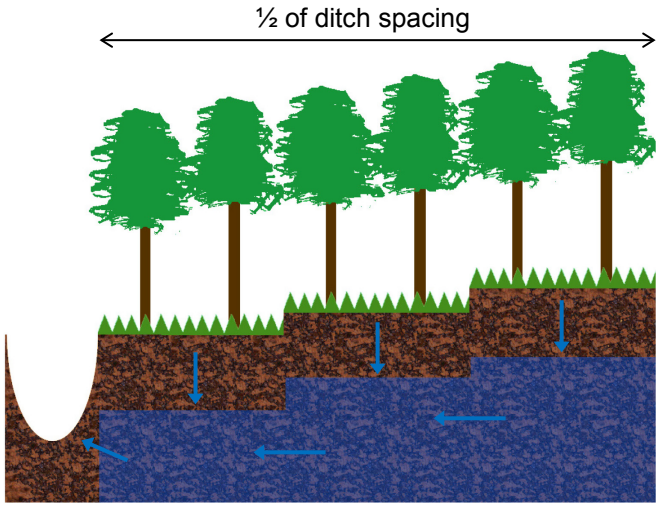

Figure 11 *Vertical and horizontal fluxes in the characteristic profile with tree soil columns.*

The hydrological model was calibrated against measured runoff at the catchment outlet and water table by adjusting the vertical and horizontal hydraulic conductivities, the coefficient of the van Genuchten (1980) model of the water retention curve and the global multiplication coefficient of potential evapotranspiration. The goodness of fit between the modeled and the measured runoff was evaluated using the Nash-Sutcliffe model efficiency coefficient which range is from –∞ to the perfect fit, 1. The chosen calibration period was 1–31 July 2012 and validation period 1–31 August 2012.

4.2 Defining network characteristics

The channels and the vertices in the network were numbered without using any specific numbering scheme (Figure 12). The length of the branches varied from 16 m (channel 11) to 278 m (channel 1). The connectivity of branches at junction was stored in form of an incidence matrix (Kujita 1995). In an incidence matrix each column represents a channel and each row a vertex. The assumed flow direction was included in the matrix by giving each channel start point the value -1 and the end point the value 1. Equation (9) presents the incidence matrix corresponding to the channel network numbering and flow directions of Figure 12.

$$\boldsymbol{I}_m = \begin{bmatrix} -1 & 0 & 0 & 0 & 0 & 0 & 0 & 0 & 0 & 0 & 0 & 0 & 0 & 0 & 0 \\ 1 & 0 & 0 & 0 & 0 & 0 & 0 & 0 & 0 & 1 & -1 & 0 & 0 & 0 & 0 \\ 0 & 0 & 0 & 0 & -1 & 0 & 0 & 0 & 0 & 0 & 0 & 0 & 0 & 0 & 0 \\ 0 & 0 & 0 & 0 & 1 & 1 & 0 & 0 & 0 & 0 & 0 & -1 & 0 & 0 & 0 \\ 0 & -1 & 0 & 0 & 0 & 0 & 0 & 0 & 0 & 0 & 0 & 1 & 1 & 0 & 0 \\ 0 & 1 & 0 & 0 & 0 & 0 & 0 & 0 & 1 & -1 & 0 & 0 & 0 & 0 & 0 \\ 0 & 0 & 0 & 0 & 0 & -1 & 0 & 0 & 0 & 0 & 0 & 0 & 0 & 0 & 0 \\ 0 & 0 & -1 & 0 & 0 & 0 & 0 & 0 & 0 & 0 & 0 & 0 & -1 & 1 & 0 \\ 0 & 0 & 1 & 1 & 0 & 0 & 0 & 0 & -1 & 0 & 0 & 0 & 0 & 0 & 0 \\ 0 & 0 & 0 & 0 & 0 & 0 & -1 & 0 & 0 & 0 & 0 & 0 & 0 & 0 & 0 \\ 0 & 0 & 0 & 0 & 0 & 0 & 1 & 1 & 0 & 0 & 0 & 0 & 0 & 0 & -1 \\ 0 & 0 & 0 & -1 & 0 & 0 & 0 & 0 & 0 & 0 & 0 & 0 & 0 & -1 & 1 \\ 0 & 0 & 0 & 0 & 0 & 0 & 0 & -1 & 0 & 0 & 0 & 0 & 0 & 0 & 0 \\ 0 & 0 & 0 & 0 & 0 & 0 & 0 & 0 & 0 & 0 & 1 & 0 & 0 & 0 & 0 \end{bmatrix} \quad (9)$$

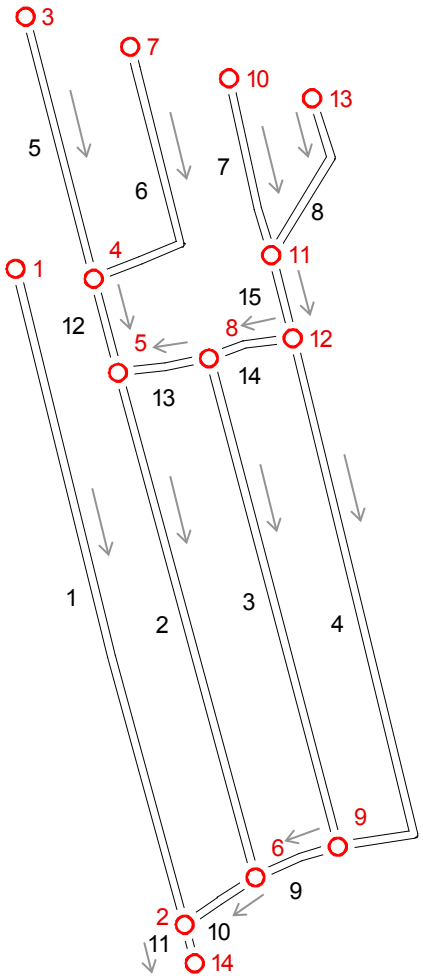

Figure 12 *Numbering of the channels (in black) and the vertices (in red) of the ditch network of the Koivupuro nested catchment.*

The maintained ditches were cleaned using a shovel which dimensions determined the shape of the channel cross-section (Figure 13). The sides of the cross-section were approximated as arcs of a circle (r = 1.355 m). Using this assumption the spread (T), the cross-sectional flow area (A) and the wetted perimeter (P) were determined as functions of flow depth (h) (Figure 13; Equations (10)–(12)).

$$T(h) = 2\left(\sqrt{r^2 - (H-h)^2} - r + \frac{L_2}{2}\right) \tag{10}$$

$$A(h) = L_1 \cdot h + 2\int_a^b \sqrt{r^2 - \delta^2}\,\mathrm{d}\delta - (H-h)(T-L_1) \tag{11}$$

$$P(h) = L_1 + 2 \cdot \int_a^b \frac{r}{\sqrt{r^2 - \delta^2}}\,\mathrm{d}\delta \tag{12}$$

where L_1 [m], L_2 [m], H [m] and r [m] are dimensions of the cross-section (Figure 13) and the integration interval is determined by a [m] and b [m] as follows:

$$a = -\sqrt{r^2 - (H - h)^2} \qquad b = \frac{L_2 - L_1}{2} - r \qquad (13–14)$$

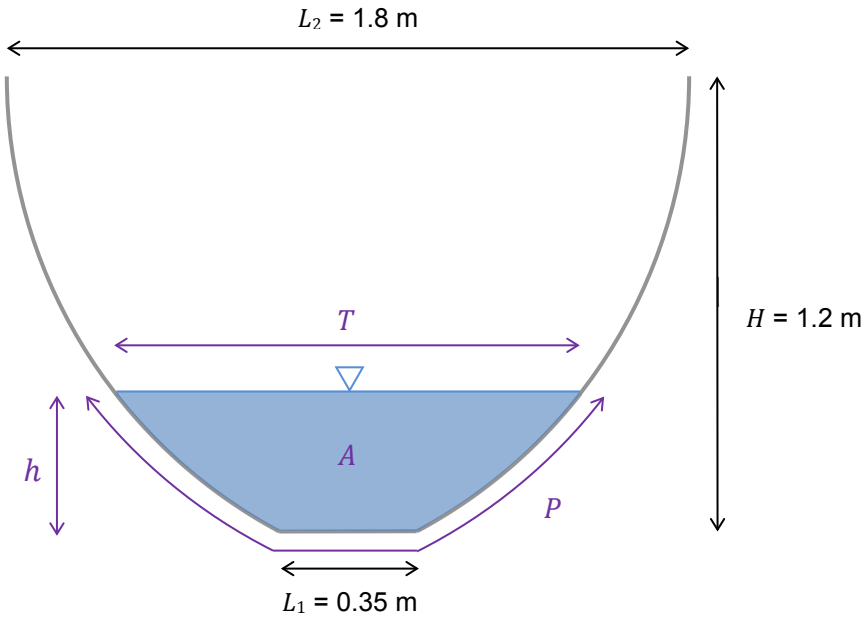

Figure 13 *Channel cross-section of the Koivupuro ditches determined by the shovel used for ditch cleaning in August 2011.*

The bottom elevation along the distance of 10 m between the elevation measurement points was approximated using linear interpolation and extrapolation if needed. The processed bottom elevation data were then smoothed by the LOWESS-method (locally weighted scatter plot smoothing) using a span of 40 m (Figure 14). The smoothing reduced the local unevenness which may complicate flow computation. The average bottom slope and the length of the channels in the Koivupuro ditch network are given in Table 1.

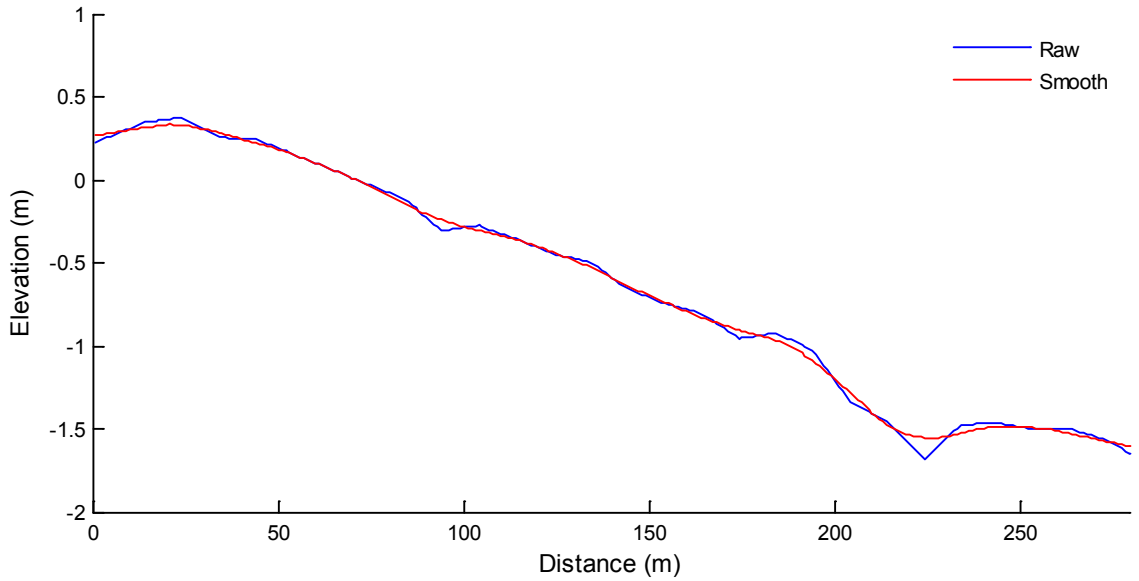

Figure 14 *Measured and smoothed (LOWESS) bottom elevation of the west most ditch (channel 1; Figure 12) of the nested catchment of Koivupuro.*

Table 1 *Channel characteristics of the Koivupuro ditch network.*

Channel number	Length (m)	Average bed slope (-)
1	278	0.007
2	215	0.006
3	207	0.007
4	241	0.007
5	111	0.020
6	122	0.015
7	74	0.008
8	72	0.008
9	36	0.006
10	35	0.002
11	16	0.004
12	40	0.006
13	38	0.015
14	35	0.002
15	35	0.022

The flow resistance in the ditches of the Koivupuro nested catchment was estimated to assess their values against Reynolds number and results reported in literature (e.g. Hosia 1980). The measured flow depths of July 2012 were used to calculate Manning's coefficient and the corresponding Reynolds number at each measurement time and each water level logger. Knowing the flow depth, the cross-sectional area and the wetted perimeter were calculated using Equations (11) and (12). Discharge at the loggers was estimated to be a certain percentage of the discharge at the outlet of the ditch network: the percentages were estimated from the modeled steady-state solution (see next section 4.3). The approximation of discharge was applied to calculate the flow velocity by dividing the discharge by the cross-sectional area. Manning's coefficient was then calculated as follows

$$n = \frac{R^{2/3} S_f^{1/2}}{v} \tag{15}$$

where R [m] is the hydraulic radius, S_f is the friction slope and v [m/s] is flow velocity. Because of limited flow depth measurements the friction slope S_f was replaced by the bed slope S_0. This led to the assumption that flow was uniform along a short reach. Reynolds number was calculated using Equation (2), where $1.3 \cdot 10^{-6}$ m^2/s was used as the kinematic viscosity of water (v_k). The chosen value for v_k corresponds to the water temperature of 10 °C (Hosia 1980).

4.3 Flow simulation in a channel network

The method proposed by Zhu et al. (2011) was used to simulate flow in the Koivupuro ditch network. The algorithm is applicable for both looped and dendritic channel networks, does not require a specific node numbering scheme and incorporates backwater effects (Zhu et al. 2011). Neither the total number of branches nor the number of

branches meeting at a junction-point were restricted in the model. The algorithm consists of an iterative procedure where flow in the channels of the network is solved separately using the Saint-Venant equations and the flow depth at the junctions are corrected at each iteration round using the characteristic method until convergence is reached (Figure 15). The algorithm was programmed using the numeric computing environment MATLAB by MathWorks.

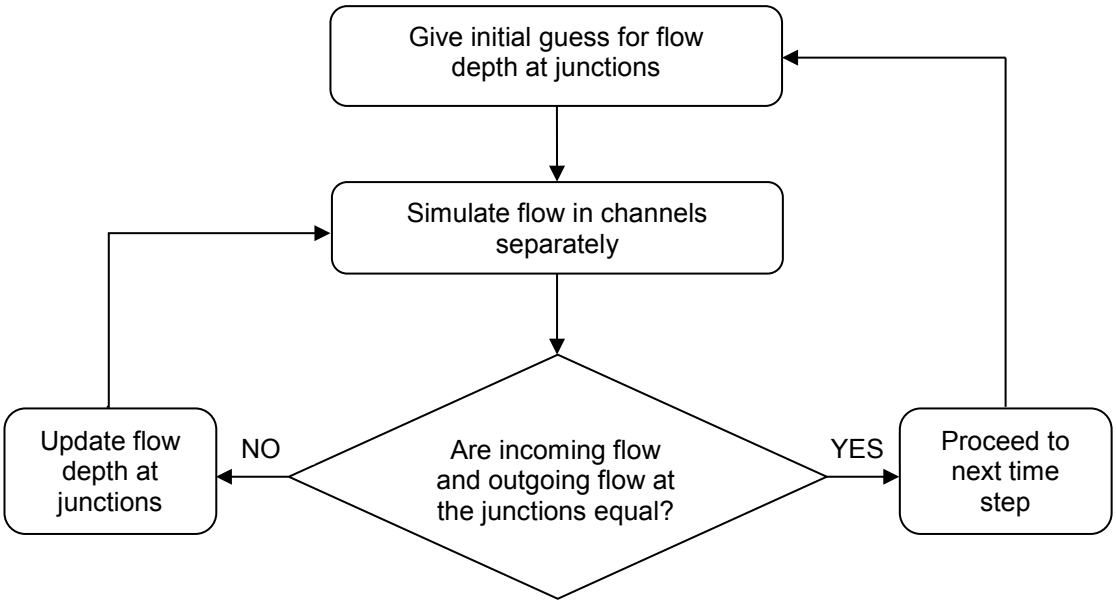

Figure 15 *Flowchart of the algorithm proposed by Zhu et al. (2011) to simulate flow in a general channel network.*

4.3.1 Discretization of governing equations

The Saint-Venant equations described in section 2.2.3 are partial differential equations and too complex to be solved by analytical methods (Cunge et al. 1980). Instead, numerical methods were required and the governing equations were discretized using an implicit finite difference method. The concept of the finite difference method is to replace the partial derivates in the equation by approximate formulas (Szymkiewicz 2010). Unlike e.g. explicit methods, implicit methods theoretically do not restrict the size of time step because of the numerical stability characteristics of the finite difference equations (Fread 1973b). Nevertheless, the computational time and distance step need to be appropriately selected: too small values lead to inefficient computation whereas too large values result in truncation errors (Fread and Lewis 1993).

In order to compute unsteady flow we are required to have an initial steady-state solution for the flow in the network. The steady-state equations are derived from the Saint-Venant equations (Equations (3) and (4)) by neglecting the time derivatives (Sen and Garg 2002; Cunge et al. 1980). To discretize the remaining longitudinal distance derivatives and the variables depending on the longitudinal distance the simple approximation formulas described by Equations (16)–(17) are used.

$$\frac{\partial f}{\partial x} = \frac{f_{i+1} - f_i}{\Delta x} \tag{16}$$

$$f = \frac{f_i + f_{i+1}}{2} \tag{17}$$

Applying these formulas to the steady-state continuity and momentum equations results in the following difference equations

$$\frac{Q_{i+1} - Q_i}{\Delta x} - q^* = 0 \tag{18}$$

$$\frac{1}{\Delta x}\left[\left(\frac{Q^2}{A}\right)_{i+1} - \left(\frac{Q^2}{A}\right)_i\right] + gA^*\frac{h_{i+1} - h_i}{\Delta x} + gn^2\left(\frac{Q|Q|}{AR^{4/3}}\right)^* - gA^*S_{0,i+1/2} = 0 \tag{19}$$

where i refers to the i^{th} node in the channel and the star-values (*) are derived using Equation (17) as follows

$$q^* = \frac{q_i + q_{i+1}}{2} \qquad A^* = \frac{A_i + A_{i+1}}{2} \tag{20–21}$$

$$\left(\frac{Q|Q|}{AR^{4/3}}\right)^* = \frac{1}{2}\left[\left(\frac{Q|Q|}{AR^{4/3}}\right)_i + \left(\frac{Q|Q|}{AR^{4/3}}\right)_{i+1}\right] \tag{22}$$

For unsteady flow the variables are both distance and time dependent forming a 2-dimensional computational grid (Figure 16). The widely used four-point Preissmann implicit scheme (Equations (23)–(25)) was chosen to discretize the full Saint-Venant equations (Cunge et al. 1980).

$$\frac{\partial f}{\partial t} = \frac{\left(f_i^{k+1} + f_{i+1}^{k+1}\right) - \left(f_i^k + f_{i+1}^k\right)}{2\Delta t} \tag{23}$$

$$\frac{\partial f}{\partial x} = \frac{\alpha\left(f_{i+1}^{k+1} - f_i^{k+1}\right) + (1-\alpha)\left(f_{i+1}^k - f_i^k\right)}{\Delta x} \tag{24}$$

$$f = \frac{1}{2}\alpha\left(f_{i+1}^{k+1} + f_i^{k+1}\right) + \frac{1}{2}(1-\alpha)\left(f_{i+1}^k + f_i^k\right) \tag{25}$$

where α is the time weighting coefficient which was set to 0.6 (Figure 16). Venutelli (2002) determined that the most suitable values for the time weighting coefficients are between 0.5 and 1. Equations (26)–(27) present the discretized form of the full Saint-Venant equations.

$$\frac{\left(A_i^{k+1} + A_{i+1}^{k+1}\right) - \left(A_i^k + A_{i+1}^k\right)}{2\Delta t} + \frac{\alpha\left(Q_{i+1}^{k+1} - Q_i^{k+1}\right) + (1-\alpha)\left(Q_{i+1}^k - Q_i^k\right)}{\Delta x} - q^{**} = 0 \tag{26}$$

$$\begin{aligned}\frac{\left(Q_i^{k+1} + Q_{i+1}^{k+1}\right) - \left(Q_i^k + Q_{i+1}^k\right)}{2\Delta t} + \frac{1}{\Delta x}\left\{\alpha\left[\left(\frac{Q^2}{A}\right)_{i+1}^{k+1} - \left(\frac{Q^2}{A}\right)_i^{k+1}\right] + (1-\alpha)\left[\left(\frac{Q^2}{A}\right)_{i+1}^{k} - \left(\frac{Q^2}{A}\right)_i^{k}\right]\right\} \\ + gA^{**}\frac{\alpha\left(h_{i+1}^{k+1} - h_i^{k+1}\right) + (1-\alpha)\left(h_{i+1}^k - h_i^k\right)}{\Delta x} + gn^2\left(\frac{Q|Q|}{AR^{4/3}}\right)^{**} - gA^{**}S_{0,i+1/2} = 0\end{aligned} \tag{27}$$

where i refers to the i^{th} node in the channel, k refers to the index of the time step and the star-values (**) are derived using Equation (25).

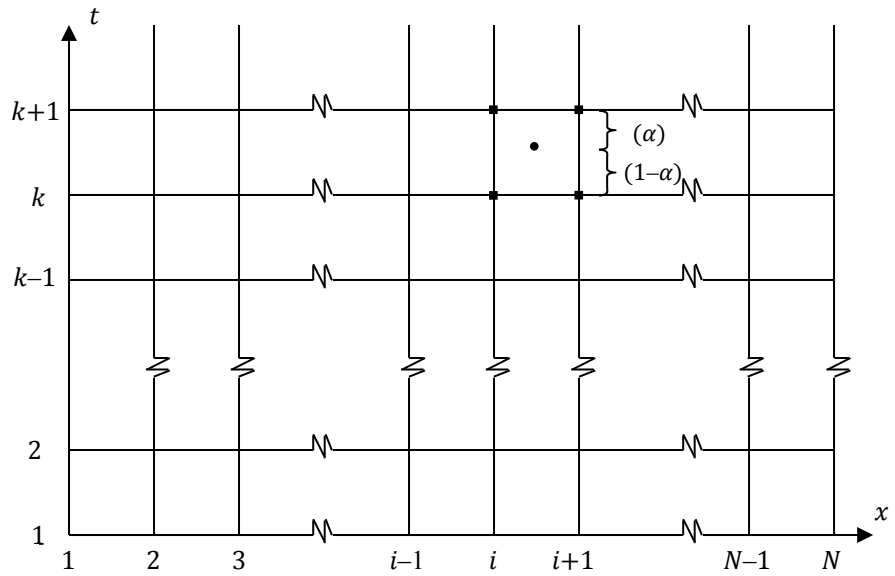

Figure 16 *Computational grid of the numerical solution of unsteady flow and an illustration of the Preissmann four-point difference scheme.*

4.3.2 Simulating flow in channels

During the iteration process the flow in each branch of the network was simulated independently using the discretized Saint-Venant equations described in the previous section. As we write the continuity and momentum equations for each reach of the channel we obtain a system of $2(N–1)$ equations, where N is the number of nodes along the channel (French 1986). However, the total number of unknowns is $2N$ (discharge and flow depth at each node) so we need two more equations to be able to solve the system of equations. These are the boundary conditions at the first and the last node, which can be either known flow depths or known discharges (Fread 1973a). Alternatively, the boundary condition can also be a known relation between flow depth and discharge.

To solve the non-linear system of equations the numerical Newton-Raphson method was applied (Szymkiewicz 2010). The Newton-Raphson method is an iterative procedure to solve a system of equations in the form

$$\boldsymbol{F}(\boldsymbol{\Phi}) = 0 \tag{28}$$

When solving flow in a channel $\boldsymbol{F}(\boldsymbol{\Phi})$ includes the upstream boundary condition on the first row then in turns the discretized continuity and momentum equations for the $N–1$ reaches ($2(N–1)$ equations) and finally on the last row the downstream boundary condition. In the case of steady-state Equations (18)–(19) are applied to the rows $2…2N–1$ of $\boldsymbol{F}(\boldsymbol{\Phi})$ and in the case of unsteady flow Equations (26)–(27) are applied to the rows $2…2N–1$ of $\boldsymbol{F}(\boldsymbol{\Phi})$. $\boldsymbol{\Phi}$ is the unknown variable vector which includes in turns Q and h for each node $1…N$.

The iterative solution starts with an initial guess for the unknown variable vector ($\boldsymbol{\Phi}$) which is corrected by an error vector ($\Delta\boldsymbol{\Phi}$) until convergence is reached (Equation (29)).

$$\boldsymbol{\Phi}_{I+1} = \boldsymbol{\Phi}_I - \Delta\boldsymbol{\Phi} = \boldsymbol{\Phi}_I - \boldsymbol{W}_I^{-1}\,\boldsymbol{F}(\boldsymbol{\Phi}_I) \tag{29}$$

where I is the index of the iteration round and $\boldsymbol{W}_I$ is the Jacobian matrix corresponding to the solution vector $\boldsymbol{\Phi}_I$. The Jacobian matrix $\boldsymbol{W}$ (Equation (30)) for the system of equations $\boldsymbol{F}(\boldsymbol{\Phi})$ needs thus to be formed and then the error vector can be calculated from Equation (31).

$$\boldsymbol{W} = \frac{\partial \boldsymbol{F}(\boldsymbol{\Phi})}{\partial \boldsymbol{\Phi}} \tag{30}$$

$$\boldsymbol{W}_I\,\Delta\boldsymbol{\Phi} = \boldsymbol{F}(\boldsymbol{\Phi}_I) \tag{31}$$

To form the Jacobian matrix $\boldsymbol{W}$ we need to differentiate the discretized continuity and momentum equations in respect to the unknown variables. The only unknowns present in the continuity and momentum equations for reach i to $i+1$ are h_i^{k+1}, h_{i+1}^{k+1}, Q_i^{k+1} and Q_{i+1}^{k+1}. The Jacobian matrix will thus contain elements only in the band along the main diagonal (Cunge et al. 1980; Figure 17). For the steady-state solution the partial derivatives of the discretized continuity (F_1) and momentum (F_2) equations in respect to h_i and Q_i are

$$\frac{\partial F_1}{\partial Q_i} = -\frac{1}{\Delta x} \qquad \frac{\partial F_1}{\partial h_i} = 0 \tag{32–33}$$

$$\frac{\partial F_2}{\partial Q_i} = -\frac{2Q_i}{\Delta x A_i} + \frac{gn^2|Q_i|}{A_i R_i^{4/3}} \tag{34}$$

$$\frac{\partial F_2}{\partial h_i} = \frac{\frac{\partial A_i}{\partial h_i}}{\Delta x}\left(\frac{Q_i}{A_i}\right)^2 + \frac{g}{2\Delta x}\left(\frac{\partial A_i}{\partial h_i}(h_{i+1} - h_i) - A_i - A_{i+1}\right) - \frac{gn^2 Q_i|Q_i|}{2A_i R_i^{4/3}}\left(\frac{\frac{\partial A_i}{\partial h_i}}{A_i} + \frac{4\frac{\partial R_i}{\partial h_i}}{3R_i}\right) - \frac{g\frac{\partial A_i}{\partial h_i}S_{0,i+1/2}}{2} \tag{35}$$

where

$$\frac{\partial A_i}{\partial h_i} = T_i \qquad \frac{\partial R_i}{\partial h_i} = \frac{T_i}{P_i} - \frac{R_i}{P_i}\frac{\partial P_i}{\partial h_i} \tag{36–37}$$

For the cross-section of Figure 13 the derivative of P_i (Equation (12)) is

$$\frac{\partial P_i}{\partial h_i} = -\frac{2r}{\sqrt{r^2 - (H - h_i)^2}} \tag{38}$$

where r [m] and H [m] are dimensions of the cross-section (see Figure 13). The partial derivatives are presented in their whole (steady-state and unsteady flow) in Appendix 1.

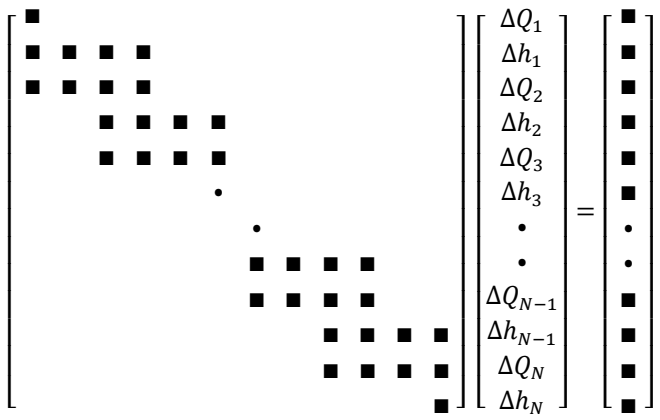

Figure 17 *Arrangement of Jacobian matrix in Equation (31) with a known discharge as upstream boundary (first row) and a known flow depth as downstream boundary (last row). The rows 2… 2N −1 include in turns* $\frac{\partial F_1}{\partial Q_1}$ $\frac{\partial F_1}{\partial h_1}$ $\frac{\partial F_1}{\partial Q_2}$ $\frac{\partial F_1}{\partial h_2}$ *and* $\frac{\partial F_2}{\partial Q_1}$ $\frac{\partial F_2}{\partial h_1}$ $\frac{\partial F_2}{\partial Q_2}$ $\frac{\partial F_2}{\partial h_2}$ *in the place of the black squares (indexes of Q and h increase to N moving down the rows).*

Because of the banded nature of the Jacobian matrix, banded matrix solution methods were used to solve the linear system of Equation (31). Finally the solution vector can be updated using Equation (29) and the procedure can be repeated until a certain tolerance for both $|\Delta Q/Q|$ and $|\Delta h/h|$ is reached.

4.3.3 Flow depth at junctions

At the junction-points of the channel network flow depth and discharge need to meet the inner boundary conditions (Equations (6) and (7)). The junction-point water stage prediction and correction method proposed by Zhu et al. (2011) is based on the characteristic method. If the predicted flow depth at the junction-point is higher than the correct value, the sum of incoming flow is lower than the sum of outgoing flow at the junction-point. The flow depth at the junctions (h_b) is corrected using the equation

$$h_{b\,K+1} = h_{b\,K} + \Delta h_b \tag{39}$$

where K is the index of the iteration round and the flow depth increment at the junctions (Δh_b) is derived from the characteristic curves according to the Saint-Venant equations resulting in

$$\Delta h_b = \frac{\sum Q_{in} - \sum Q_{out}}{\sum\left(\sqrt{g A_{in} T_{in}} - Q_{in} T_{in}/A_{in}\right) + \sum\left(\sqrt{g A_{out} T_{out}} - Q_{out} T_{out}/A_{out}\right)} \tag{40}$$

where subscript in refers to the incoming channels and out to the outgoing channels. Equations (39)–(40) are repeated until a certain tolerance is reached for $|\Delta h_b/h_b|$.

4.3.4 Programming the algorithm

The algorithm for simulating flow in a channel network was programmed using MathWorks' numeric computing environment MATLAB. A main program with numerous subprograms and custom functions was build using the MATLAB language of numerical computation. The outline of the program is presented in Appendix 2.

The program starts by reading the input data from an Excel-file. First the resolution of the simulation (Δx and Δt) and the interval at which the catchment discharge is specified in the input file (Δt_{input}) are defined. The input-file consists of

- branch lengths
- elevation of channel bottoms
- incidence matrix
- catchment discharge at a Δt_{input} interval
- lateral inflow coefficients at a Δx interval for each channel

The number of channels, vertex and nodes in each channel are computed using the incidence matrix and branch length information. The discharge data are interpolated to the interval of the discretization (Δt). Also the elevation data are interpolated, smoothed and slopes of each reach are calculated. The variables are saved in matrix format where the columns correspond to channels and the rows to nodes in the channels. Furthermore, the Manning's roughness coefficient, the boundary conditions and the cross-section dimensions are defined in the input-program.

Next the initial guesses for the flow depth at the junctions and for both discharge and flow depth at all the nodes of the network are defined in the main-program. The initial guess for the junction-point flow depths, or later in the simulation the junction-point flow depths of the previous time step, are set as the internal boundary conditions of the current time step. After this the Saint-Venant equations are solved for all the channels with an account for the internal and external boundary conditions. During each iteration round the geometry (A, P, R, T, $\frac{\partial A}{\partial h}$, $\frac{\partial P}{\partial h}$ and $\frac{\partial R}{\partial h}$) corresponding to the current flow depth needs to be recalculated at each node of the channel. This is done by a subprogram which includes the equations of these variables presented in sections 4.2 and 4.3.2.

The Jacobian matrix ($\boldsymbol{W}$) and the system of equations ($\boldsymbol{F}$) of the linear system of Equation (31) are formed using custom functions that were created for the discretized continuity and momentum equations and their partial derivates. Each function included the equations for both steady-state and unsteady flow simulation. By checking the current time step's index the correct equations were chosen. If $t = 0$ we were still solving the initial steady-state solution and if $t > 0$ unsteady flow was simulated. The boundary conditions were added to the first and last rows of $\boldsymbol{W}$ and $\boldsymbol{F}$ to keep the banded format of the Jacobian matrix. The Jacobian matrix was stored as a sparse matrix instead of a full matrix to save storage space. In a sparse matrix only the nonzero elements are saved.

The correction vector ($\Delta\boldsymbol{\Phi}$; Equation (31)) was solved using the MATLAB *mldivide*-function which uses banded matrix solution methods to solve a linear system when the coefficient matrix is banded. The solution vector ($\boldsymbol{\Phi}$) was then updated following Equation (29). In the case of negative values of flow depth and complex values of discharge the solution vector was filtered such that $h = |h|$ and $Q = \text{Re}(Q)$. This prevented the

solution from aborting due to instability. A *while*-loop was applied to carry on the iteration procedure until $|\Delta Q/Q|$ and $|\Delta h/h|$, i.e. $|\Delta \boldsymbol{\Phi}/\boldsymbol{\Phi}|$ reached the desired tolerance. Before proceeding to the next channel in the network Q and h were stored to be used as an initial guess of the next iteration round. Each channel in the network was solved by applying a *for*-loop.

When flow was solved in each channel of the network the Equations (39)–(40) were applied to correct the flow depth at the junction-points. Again a *while*-loop was applied to carry on the iteration process of the junction-point flow depths until $|\Delta h_b/h_b|$ for all junctions reached the defined tolerance. When convergence was reached, i.e. the solution for the current time step was found, the result and the geometry (Q, h, A, R and T) for the current time step were stored and the algorithm proceeded to the next time step. As a summary, the loops included in the algorithm are the following

```
FOR time < t_max
    ⋮
    WHILE |Δh_b/h_b| > tolerance
        ⋮
        FOR channel 1... M
            ⋮
            WHILE |ΔΦ/Φ| > tolerance
                ⋮
            END
            ⋮
        END
        ⋮
    END
    ⋮
END
```

After simulating flow for the last time step the results are stored in a MATLAB-file.

4.3.5 Model application and evaluation

In the model applications the flow at the upstream boundaries was set to zero and a relation between discharge and flow depth was specified at the downstream boundary. All the flow entering the channels was through lateral inflow. A tolerance of 0.001 for $|\Delta Q/Q|$, $|\Delta h/h|$ and $|\Delta h_b/h_b|$ was set for all the simulations. Alternatively, convergence was assumed when values of Q or h were smaller than 10^{-10}. An additional restrain was set to the junction-point flow depth by checking if the sum of incoming flow really matched the sum of outgoing flow. To initiate the iterative procedure an initial guess of constant flow depth and discharge in the whole channel network was specified.

To experiment on model performance the model was applied to numerous simple 3- and 6-channel networks with varying discharge, bed slopes, channel lengths and grid resolutions. Finally the model was applied to the actual ditch network of the Koivupuro nested catchment. The boundary condition at the outlet of the network was set by the known relationship between discharge and flow depth determined by the V-notch weir:

$$Q = 1.381(h - h_{weir})^{5/2} \quad (41)$$

where Q [m^3/s] is discharge, h [m] is flow depth at the weir and h_{weir} [m] is the distance from the bottom of the ditch to the bottom of the V-notch. The grid resolution of $\Delta x = 1$ m and $\Delta t = 900$ s was chosen for the application of the model. First the measured discharge at the catchment outlet was used as the lateral inflow variable and then further simulations were conducted with the computed runoff of the FEMMA-model. Linear interpolation was used to estimate the model input discharge at an interval corresponding to the chosen simulation time step.

The flow depth profiles computed by the model were compared to the measured flow depths at the water level measurement points (Figure 8) during a 20 day long period in July 2012. The modeling period included the highest flow event of the summer months of 2012 and several other lower flow events (see Figure 10). Different Manning's roughness coefficients were experimented to gain better understanding of the behavior of flow resistance in small streams. No actual calibration for the whole modeling period was conducted because of the obvious variation of flow resistance during changing flow conditions.

4.4 Evaluation of potential erosion

The critical parts of the network in terms of erosion were localized by means of bed shear stress. Bed shear stress was calculated at each node of the network over the whole simulation period using Equation (42):

$$\tau_b = \rho g \frac{v^2 n^2}{R^{1/3}} \quad (42)$$

where ρ [kg/m^3] is the density of water. The bed shear stress values were compared to the critical shear stress reported for a drained Finnish peatland site by Marttila and Kløve (2008). When the bed shear stress exceeds the critical value (τ_{cr} = 0.059 N/m^2) erosion starts to occur and thereafter the higher the bed shear stress the greater the erosion rate (Marttila and Kløve 2008).

On the other hand computed flow velocity values were compared to reported critical values. Table 2 summarizes critical velocity values reported for Finnish peatland sites.

Table 2 *Critical flow velocities for erosion of the peat layer reported in Finnish studies.*

Publication	Critical velocity for surface layer of peat (m/s)	Critical velocity for the whole peat layer (m/s)
Marttila and Kløve (2008)	0.06	0.15
Heikkinen (2004)	0.08	-
Kløve (1998)	0.04	-
Aho and Kantola (1985)	0.15	-

5 Results and discussion

5.1 Runoff to ditches at Koivupuro

Calibration of the hydrological FEMMA model led to a Nash-Sutcliffe coefficient of 0.69 for the period 1–31 July 2012. Despite calibration, the model tended to consistently underestimate high flow peaks and overestimate low flow peaks (Figure 18a). The reason why the highest flow peaks are not reached may be due to the hourly resolution of the input precipitation data. In reality an intensive precipitation event probably lasts for a shorter time period than 1 hour. In addition the precipitation was measured on a different location (3 km away) which might account for some of the differences. For the calibration period, July 2012, the computed water balance was runoff centered (54 %) while interception and transpiration by the vegetation accounted for 39 %. The results of model validation are shown in Figure 18b. The validation period produced a Nash-Sutcliffe coefficient of 0.75.

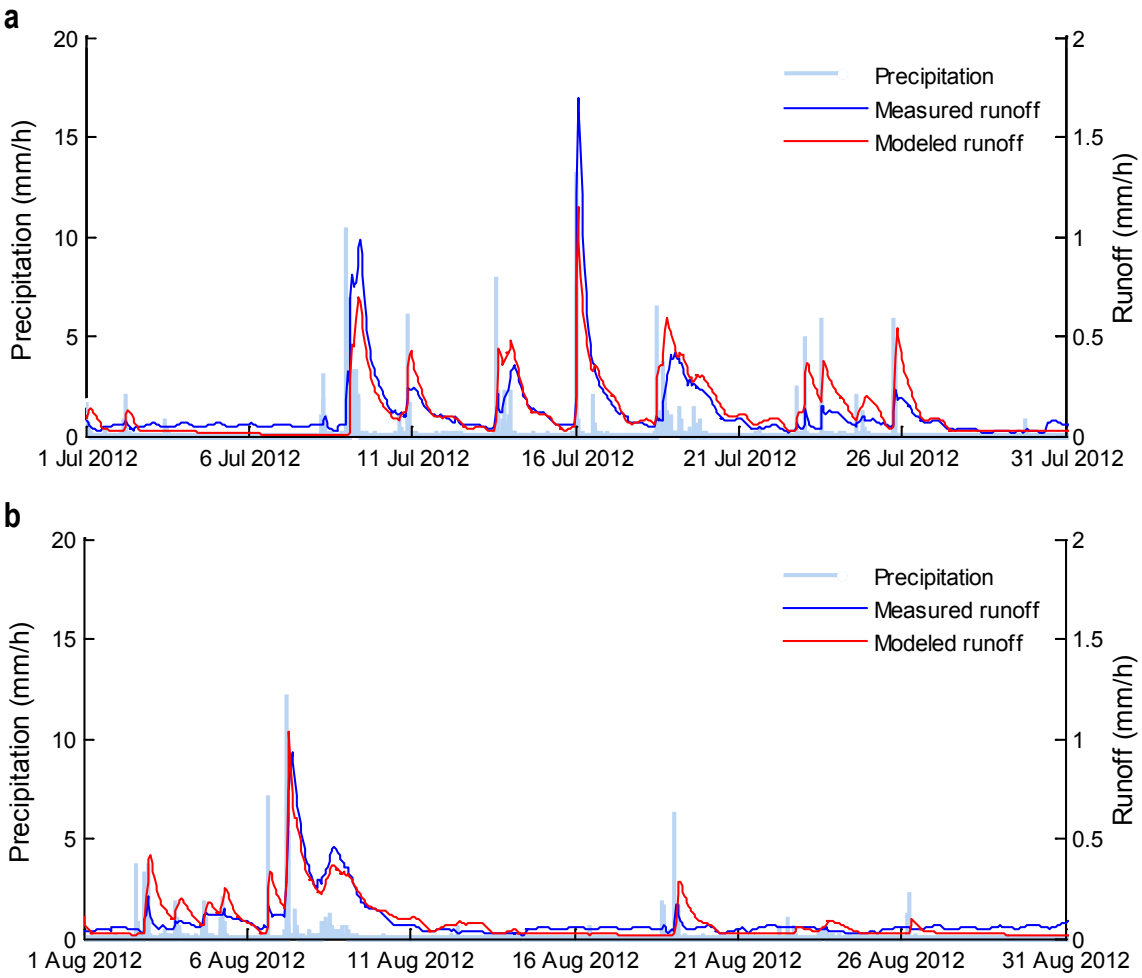

Figure 18 *Modeled and measured runoff of the Koivupuro nested catchment during the calibration period (a) and the validation period (b), and the precipitation used as model input measured at Iso-Kauhea (located 3 km from the Koivupuro catchment).*

The results of flow accumulation into the ditches at a 1 m interval are illustrated in Figure 19. Although the applied D8-method is widely used, it may result in inaccurate results since there is no possibility for flow to be distributed to two directions or in a di-

rection somewhere between the eight possible directions (Seibert and McGlynn 2006). However, in the case of the Koivupuro nested catchment a bigger restrain is probably caused by the rather coarse grid resolution of the elevation raster (10×10 m^2). Also it might be unrealistic that a large amount of flow would enter the ditch at a distinct point rather than more evenly along a longer reach.

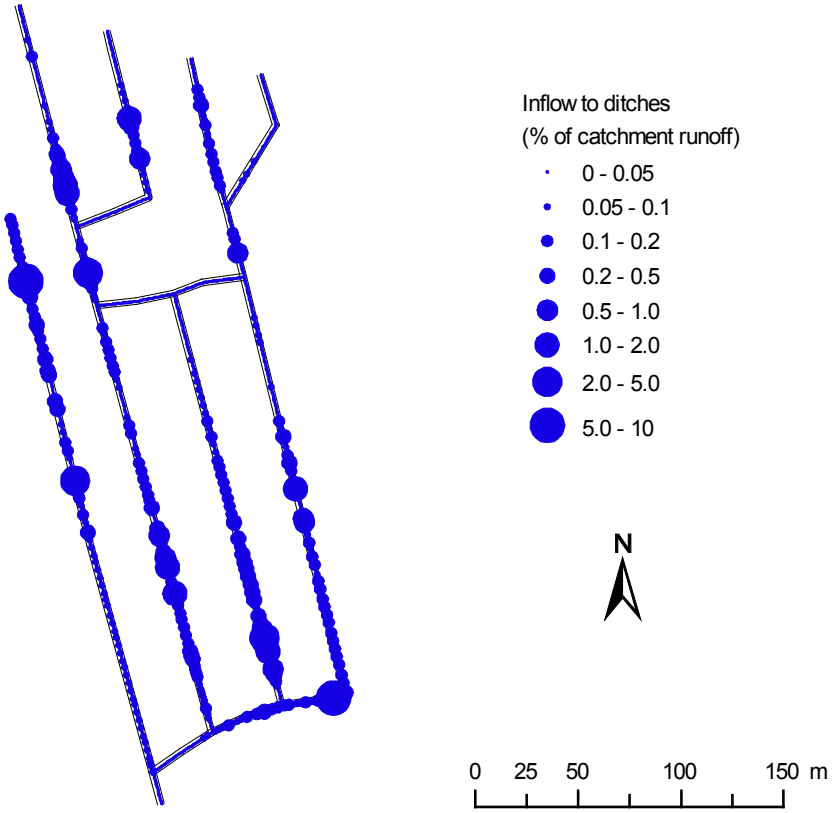

Figure 19 *Inflow to ditches at the Koivupuro nested catchment calculated using the D8 single flow direction algorithm.*

5.2 Flow resistance evaluation

The Manning's coefficient calculated for the ditches in the Koivupuro nested catchment according to the measured flow depths (section 4.2) ranged from 0.2 to up to 10. These values are considerably higher than the values reported for peatlands in literature. Reports from Finnish drained peatland sites have determined or applied Manning's roughness coefficients in the range of 0.02–0.04 (Hosia 1980; Marttila and Kløve 2008; Tuukkanen 2010; Lappalainen et al. 2010). The larger Manning's coefficients of the Koivupuro ditches are explainable through the small cross-sectional area and the low flow magnitudes. The Manning's coefficients calculated here do not account only for the roughness of the peat bed but also all other energy losses caused by e.g. the variation of the cross-section and of the bottom slopes, micromeandering and singular roughness elements.

A clear relationship between Reynolds number and Manning's resistance coefficient was observed for the ditches at Koivupuro (Figure 20). The Manning's coefficients calculated for logger 1 were not included in Figure 20 because the damming effect of the weir at the outlet reached logger 1, which broke the assumption of uniform flow

($S_f \neq S_0$). The calculated Manning's coefficients fitted well among the results reported by Hosia (1980) for Finnish earth channels (Figure 20). Between $10^3 \leq Re \leq 10^4$, where the Reynolds numbers coincided the calculated Manning's coefficients for the Koivupuro ditches appeared between the two extremes (curvy earth channel with vegetation and recently dug earth channel). Also with lower Reynolds numbers the points formed a reasonable extension to the reported curves by Hosia (1980). It also appeared that by means of extrapolation flow with a high Reynolds number (e.g. 10^5) in the Koivupuro ditches would result in a Manning's coefficient that is in accordance with the values reported in literature (n = 0.02–0.04). No such high flow events have however been recorded in the Koivupuro ditch network so this could not be verified.

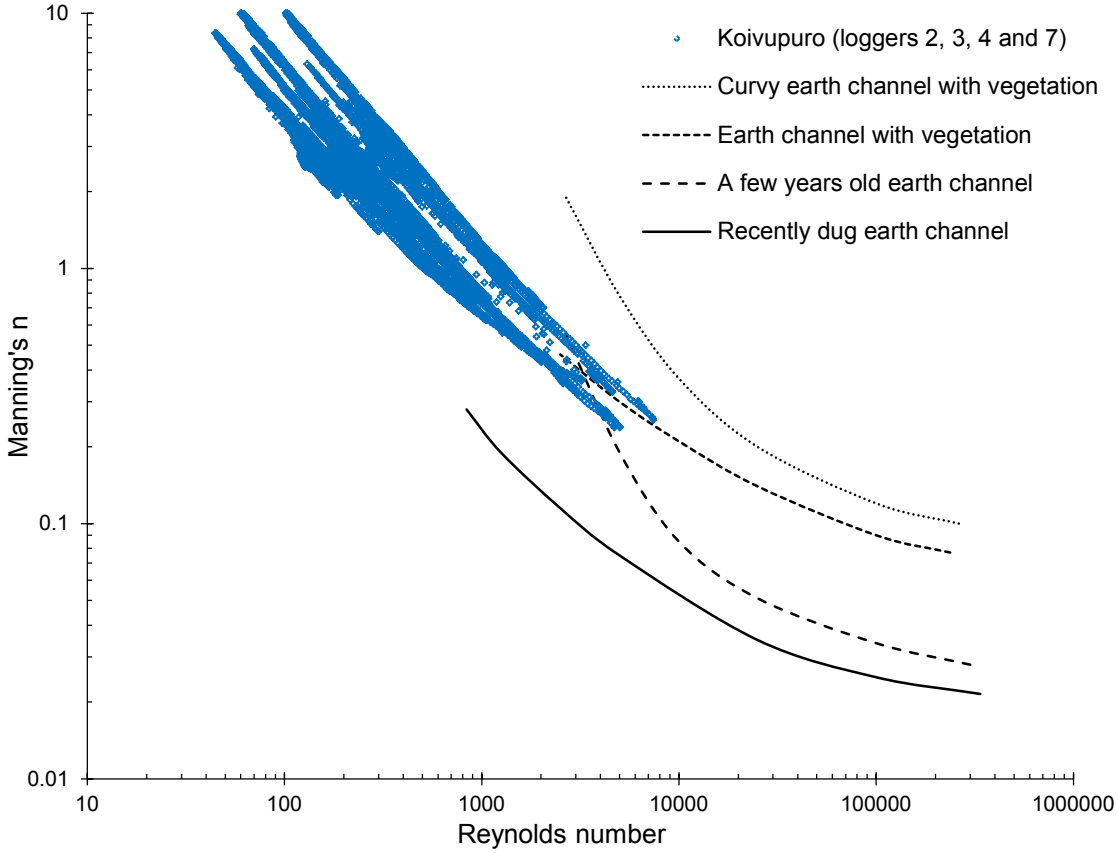

Figure 20 *The estimated Manning's resistance coefficients against Reynolds number in the ditches of the Koivupuro nested catchment and (Re, n)-relations reported by Hosia (1980) for different small scale earth channels in Finland.*

The measured flow depths used in this evaluation were produced using the average of the logger leveling measurements of the years 2011 and 2013. The applied flow depths were thus subject to some error because there were no leveling measurements of the year 2012 available. Furthermore, additional uncertainty was added by the difficulty of determining the actual location of the bed of the ditches. Peat as bed material has a very high porosity (according to Walczak et al. (2002) up to 90 %) creating potentially a soggy layer with a high water content on the bed of the ditch. It might be that the flow depth measurements included some centimeters of the soggy bottom layer, since measurements of the ditch bottoms have been determined with a rather heavy leveling staff. The leveling staff may have sunk into the bottom material causing a consistent error in the measured flow depths. If the actual flow depth were slightly lower the Reynolds

numbers would be higher and Manning's n lower which would move the points of Figure 20 slightly towards the bottom right corner.

5.3 Flow simulation in the Koivupuro ditch network

5.3.1 Model performance

Grid resolution

The Preissmann four-point implicit scheme applied in the algorithm has been reported to be stable for any Courant number, meaning there are no requirements for the relationship between Δx and Δt except for the restriction on the time weighting coefficient $\alpha \geq 0.5$ (Szymkiewicz 2010). However, it was observed that inappropriate or too large grid resolution produced unrealistic values such as negative flow depths which eventually prevented convergence of the algorithm. According to Fread and Lewis (1993) unrealistic results due to inappropriate grid resolution may cause computer programs of implicit dynamic routing models to abort. To avoid unrealistic results a filter was set in the algorithm to ensure that flow depth remained positive, as described in section 4.3.4.

Still after setting the filter for flow depth, unrealistic solutions were detected in the form of spurious spikes in flow depth along a single channel as Δx increased (Figure 21). Similar effects of too large values for grid resolution on simulation results have been reported by Fread and Lewis (1993). The unreality of the results came up when the discharge and flow depth were low and especially at the location close to the downstream boundary.

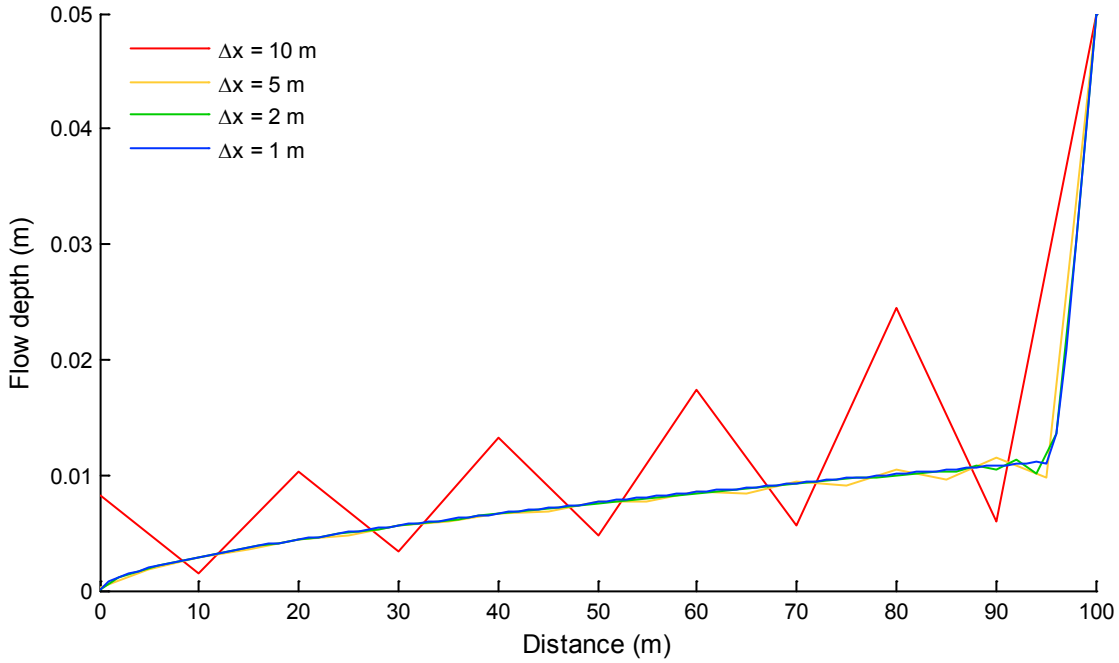

Figure 21 *Steady-state flow depth along a single channel with decreasing Δx when the downstream boundary was 0.05 m and lateral inflow was constant at each node ($S_0 = 0.01$, $n = 0.05$, $\Delta t = 5$ min).*

Solutions obtained from the implicit difference equations have been mathematically shown to converge to the true solutions of the Saint-Venant equations as Δx and Δt approach zero (Fread 1973b). On the other hand finer grid resolution decreases computa-

tional efficiency (Fread 1973b), thus finally choosing an appropriate grid resolution is about finding a balance between minimizing discretization error and maximizing computational efficiency. The final grid resolution chosen for the model application at the Koivupuro ditch network was roughly in accordance with the empirical selection criteria reported by Fread and Lewis (1993):

$$\Delta t = \frac{T_r}{20} \qquad \Delta x \leq c\frac{T_r}{20} \tag{43–44}$$

where T_r [s] is the hydrograph's time of rise and c [m/s] can be approximated as the kinematic wave celerity $c = k'v$, where k' is 3/2 for most natural channels and v [m/s] is the flow velocity. During the modeled time period, the time of rise of the major flow event was approximately 3.5 hours. Although the empirical criterion of Fread and Lewis (1993) suggest the use of Δt = 10.5 min, for the sake of computational time and comparing modeled results to measurements the time step was set at Δt = 15 min. The distance step had to be set very small (Δx = 1 m) to avoid spikes in the computed flow depths along the channels with low flow rates.

Applicability of model

Application to the Koivupuro ditch network showed that the build model produced stable and realistic results. The simulated flow depths were continuous and smooth: no physically impossible jumps in depths were observed along channels or at junctions of the network (Figure 22, Appendix 3). Another important matter regarding flow simulation in channel networks is the conservation of mass at the junction-points. Figure 23 demonstrates how the simulated flow entering a junction was equal to the simulated flow exiting a junction.

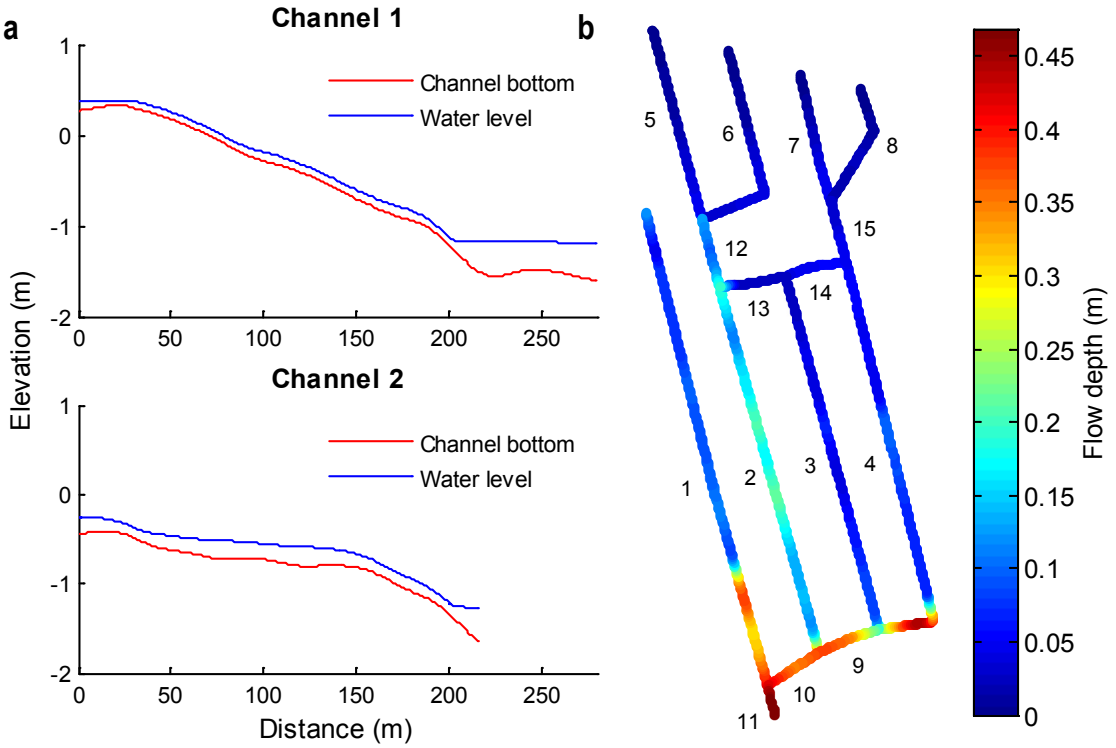

Figure 22 *Flow depth during the peak flow rate in ditches 1 and 2 of the Koivupuro ditch network (a; for all ditches see Appendix 3) and in the whole channel network (b).*

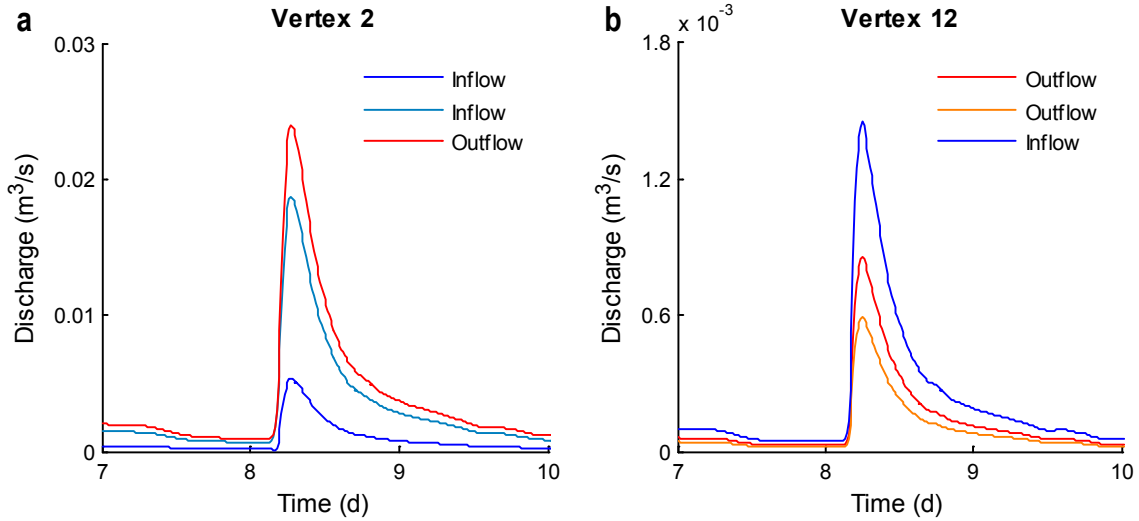

Figure 23 *Conservation of mass at a diverging junction (a) and a converging junction (b) of the Koivupuro ditch network during the highest flow peak (notice different discharge range between a and b).*

Model running time

All the computations were run on an Intel Core2 Quad Q9400 computer. When the time step of Δt = 15 min was used, the solution of a single time step took up to 130 seconds (Figure 24). On average the time needed for unsteady flow simulation in the network at one time step was 11 s. Changes in the input discharge led to longer running times as the initial guess, i.e. the solution of the previous time step, deviated more from the solution of the current time step (Figure 24). A remarkable addition to the running time was the solution of the initial steady-state flow which took up to 4 minutes. The computation time was of course dependent on the initial guess for flow depth and discharge in the

network. Figure 25 shows how fixing the junction-point flow depths starting from a simple initial guess (h_b = 0.1 m) took almost 370 iterations. For the following unsteady flow simulation one time step needed on average 14.1 iterations. Zhu et al. (2011) reported they needed on average 1.6 iterations per time step to simulate unsteady flow. The number of iterations is however in close relation to the chosen time step, the characteristics of the network and the inflow hydrograph.

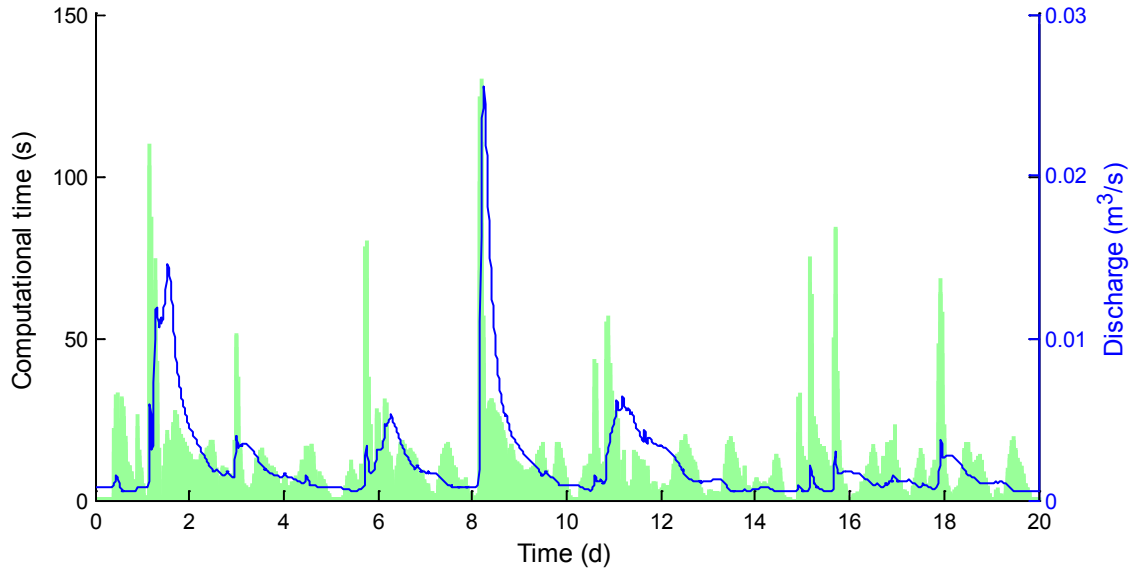

Figure 24 *Computational time needed for the iterative solution of unsteady flow at each time step for the Koivupuro ditch network and the discharge at outlet of the catchment (Δt = 15 min).*

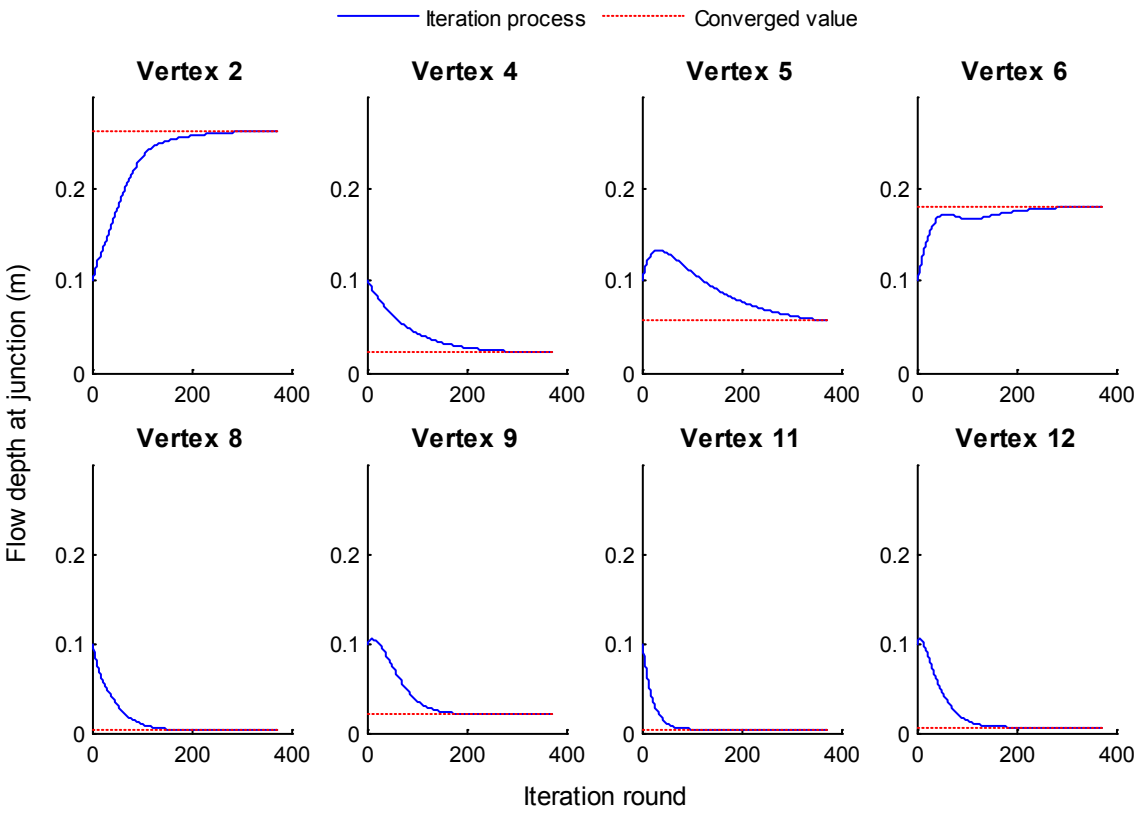

Figure 25 *Convergence of the junction-point flow depth prediction and correction algorithm (Zhu et al. 2011) for steady-state flow simulation in the Koivupuro ditch network.*

All together the simulation time for a 20 day long period was about 6 hours. The high running time was mainly due to the complexity of the network (15 branches, 2 loops) and the fact that we were forced to use a small distance step (Δx = 1 m) leading up to almost 300 nodes in some of the branches. Also the lateral inflow included in the model may contribute to the longer running time (Niemi 2010). Table 3 shows that the length of the time step also affects the running time. On one hand the running time of a single time step decreases with decreasing Δt because of the initial guess being closer to the solution. On the other hand the total simulation time increases with decreasing Δt because the number of the time steps increases.

Table 3 *Effect of the size of the time step on the running times of the unsteady flow simulation in the Koivupuro ditch network.*

Length of time step (min)	Number of time steps (-)	Average running time per time step (s)	Total simulation time (h)
5	5761	6.4	10.26
10	2881	9.2	7.37
15	1921	11.2	5.98
30	961	16.9	4.52

Despite the long running time of the model experienced in this application, Zhu et al. (2011) have experimentally shown that the present algorithm is very compatible and faster in running time compared to other algorithms (e.g. Sen and Garg 2002). The channel networks modeled by Zhu et al. (2011) were however far simpler than the Koivupuro ditch network. The networks had a maximum of one loop, the number of nodes per channel was no more than 37 and the networks had no lateral inflow along the channels. In the case of the Koivupuro ditch network the advantage of the applied algorithm of Zhu et al. (2010) compared to the algorithm of Sen and Garg (2002) may be less significant since the ratio of the number of branches to the total number of nodes in the network was very small, ca. 0.01. Considerable savings on running time could however be achieved by parallel processing, since in the algorithm flow simulation in each branch of the network is independent from the other branches.

5.3.2 Flow simulation results

When the model was run with a small Manning's coefficient the results suggested that flow resistance should be significantly higher (Figure 26). The measured flow depths are presented as bands in Figure 26 (and from here on) since there was large uncertainty in the level of the bed of the ditches at the measurement points. According to the ditch bottom leveling measurements in 2011 and 2013 error limits for the measured flow depth were established. At each logger the modeled flow depth was up to 0.1 m shallower than the measured flow depth when Manning's n = 0.08. Nevertheless, the differences in flow depth profiles between the measurement locations were well captured by the model. This means that at logger 1 where the measured flow depth was the highest the flow depth produced by the model was also the highest and so forth. The consistent flow depth results are due to the results of successful description of bottom slopes and flow distribution into the network. Manning's n = 0.08 was the smallest roughness coefficient that the model could handle for the ditch network of the Koivupuro nested

catchment. With smaller n problems arose in the steepest ditch (number 15; Table 1) during low flow conditions. It might be that flow turned from subcritical to supercritical at this point or that flow depth was so shallow that the distance step (Δx = 1 m) was not sufficient.

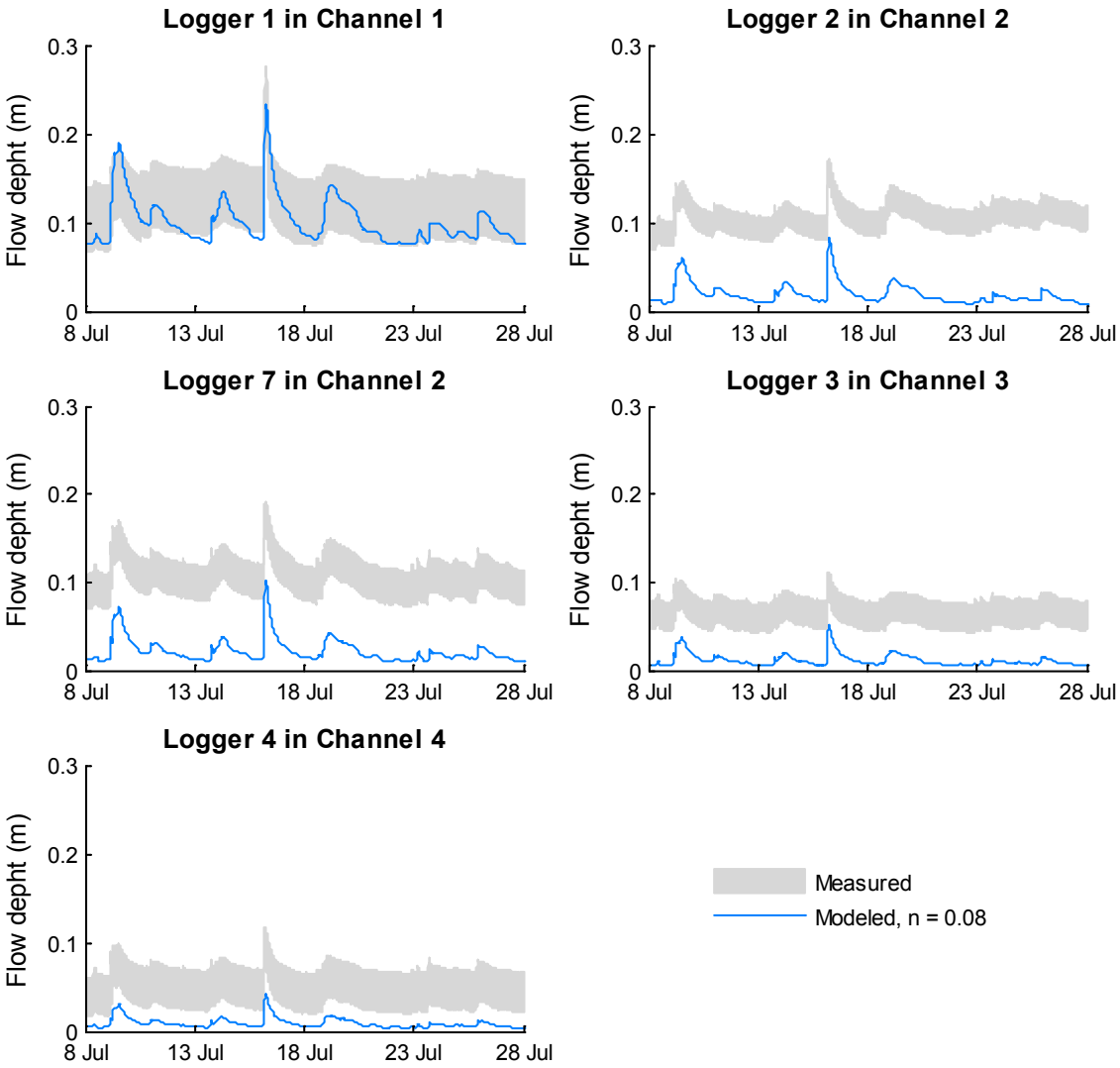

Figure 26 *Modeled flow depths with n = 0.08 and the error limit range of the flow depth measured by the loggers in the Koivupuro ditch network in July 2012 (see Figure 8 for location of loggers).*

Consequently flow was simulated using Manning's $n \geq 0.2$ as suggested by the evaluation in section 5.2. Higher flow resistance coefficients resulted in higher flow depths (Figure 27). At logger 1 in channel 1 the variation of Manning's n did not have as big an effect because of the damming effect of the weir at the outlet of the catchment. Figure 27 illustrates how flow depths during the peak flows can be reached with Manning's n in the range of 0.2–0.6 but that during low flows even higher n would be needed. Depending on the logger the highest flow peak was reached with $0.2 \leq n \leq 0.3$, the second highest with $0.3 \leq n \leq 0.5$ and the smaller ones with $n \geq 0.5$. This seemed to be in good accordance with the relationship between Reynolds number and flow resistance determined in section 5.2. At loggers 3 and 4 where less water was flowing, thus having a smaller Reynolds number, a higher Manning's n was required to reach the measured

flow depths compared to the loggers in channel 1 and 2. On the other hand the higher the flow peak was, the smaller the required resistance coefficient was.

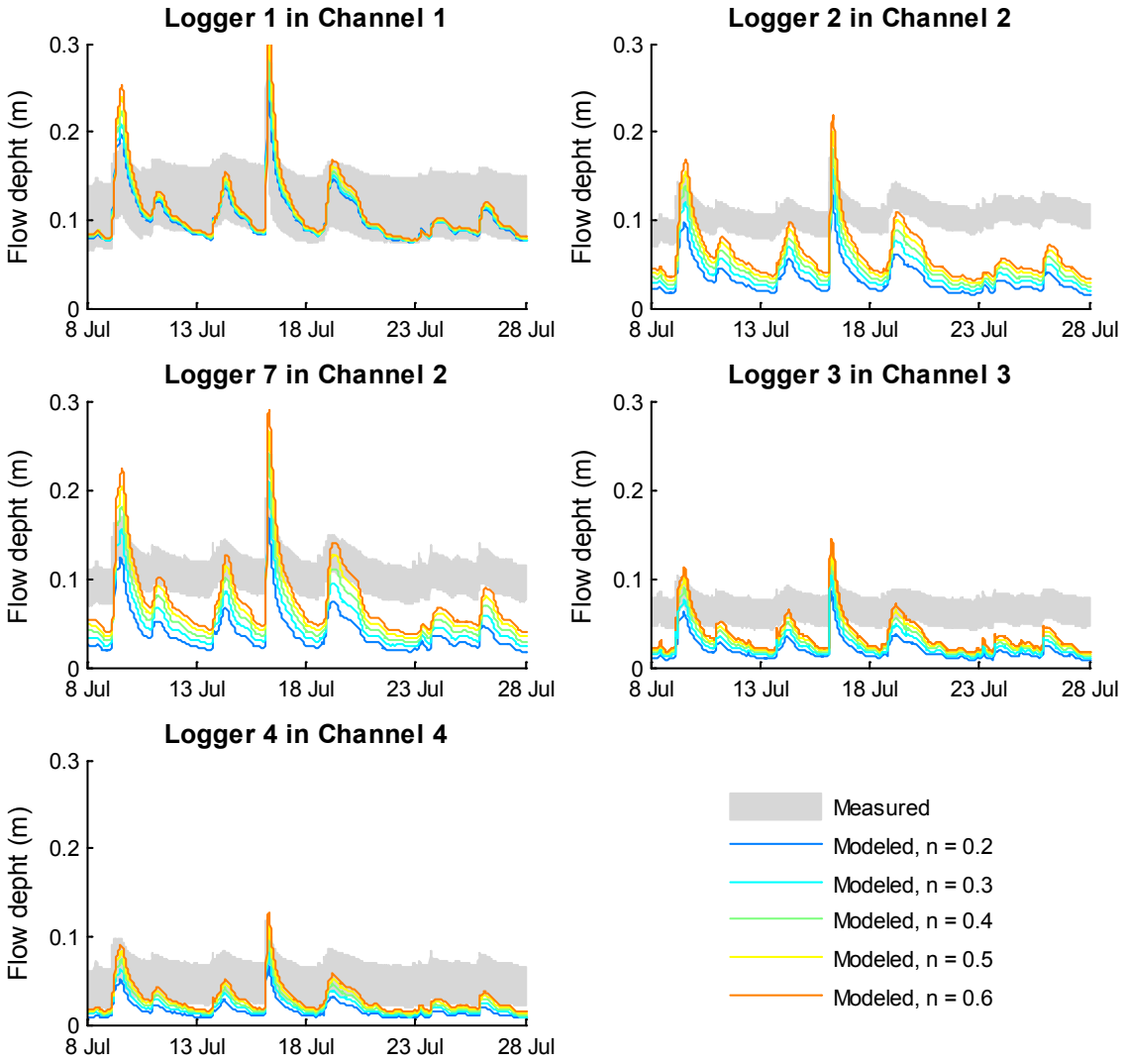

Figure 27 *Modeled flow depths with $n \geq 0.2$ and the error limit range of the flow depth measured by the loggers in the Koivupuro ditch network in July 2012 (see Figure 8 for location of loggers).*

The required resistance coefficient thus varied spatially and in time, which sets a real challenge to modeling flow in a network of this type over the full range of flow conditions. Small drainage ditches differ from the regular flow modeling targets, i.e. larger scale rivers and canals, where laminar inflow can often be neglected (Niemi 2010). In large scale channels discharge is high all along the water course while in the ditch network of Koivupuro we have almost no flow in the upstream part and considerably higher flow close to the outlet caused by lateral inflow. Contrary to flow simulation in a large scale water courses, modeling flow in small streams obviously demands a varying flow resistance. In the case of the entire ditch network of the Koivupuro nested catchment it will however not be sufficient to vary Manning's n with time according to the magnitude of the occurring flow because there are also large differences in discharge within the network. Implementing the relationship between Reynolds number and flow resistance presented in section 5.2 would be required to be able to simulate flow during

a period with varying flow in the ditch network of Koivupuro. However, including this into the flow model would be challenging since it may easily lead to instability issues.

Modeling experiments showed that a Manning's coefficient of the magnitude of 3 would be needed to reach the measured flow depths during low flow conditions. In the scope of this work no reports of such high values were found in literature. However it has been reported before that Manning's coefficient may increase by almost one order of magnitude when flow depth decreases (Asano and Uchida 2011). Asano and Uchida (2011) reported a Manning's n as high as 1.88 for a small steep mountain stream in Japan. In comparison to the manmade regular ditches in the Koivupuro catchment it seems rather inappropriate to use a Manning's n even higher than the one measured in a highly irregular mountain stream. This raises the question whether there are sources of error causing the false estimation of such high Manning's n like for instance the challenges in flow depth measurements as discussed in section 5.2 and the uncertainty of the actual cross-sectional area.

On the other hand, the interest of flow simulation usually is not on the low flow conditions but on the flow peaks related to spring snow melt or precipitation events. It would thus only be necessary to get though the low flow conditions without computational difficulties so that longer time periods could be simulated. In the Koivupuro application stable simulation of low flow conditions was assured by setting the distance step very short. Simulation of low flow conditions could however be handled in a more efficient way, e.g. by adding a low flow path to the cross-section which would probably allow a longer distance step reducing the amount of computational nodes.

A possible source of error to the modeled flow depth profiles could be the assumed constant cross-section of the ditches. Although the ditches are recently cleaned to a relatively regular cross-section flow is likely to have shaped the bottom of the ditches and the fairly steep walls of the ditches may have collapsed here and there. In the model the cross-section had a horizontal bottom width of 0.35 m, which meant water always flowed in the ditches at a minimum spread of 0.35 m. In reality flow of a couple of centimeters deep would not spread across 0.35 m but more likely across 0.05 or 0.10 m. An experiment of narrowing the horizontal bottom width to 0.05 m (Figure 28) shows how the flow depth rises rather consistently by about 0.02 m (Figure 29).

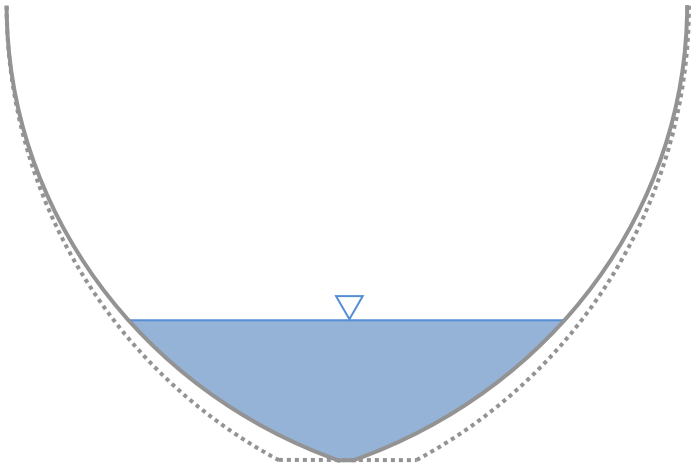

Figure 28 *Modified cross-section as continuous line and original cross-section as dashed line.*

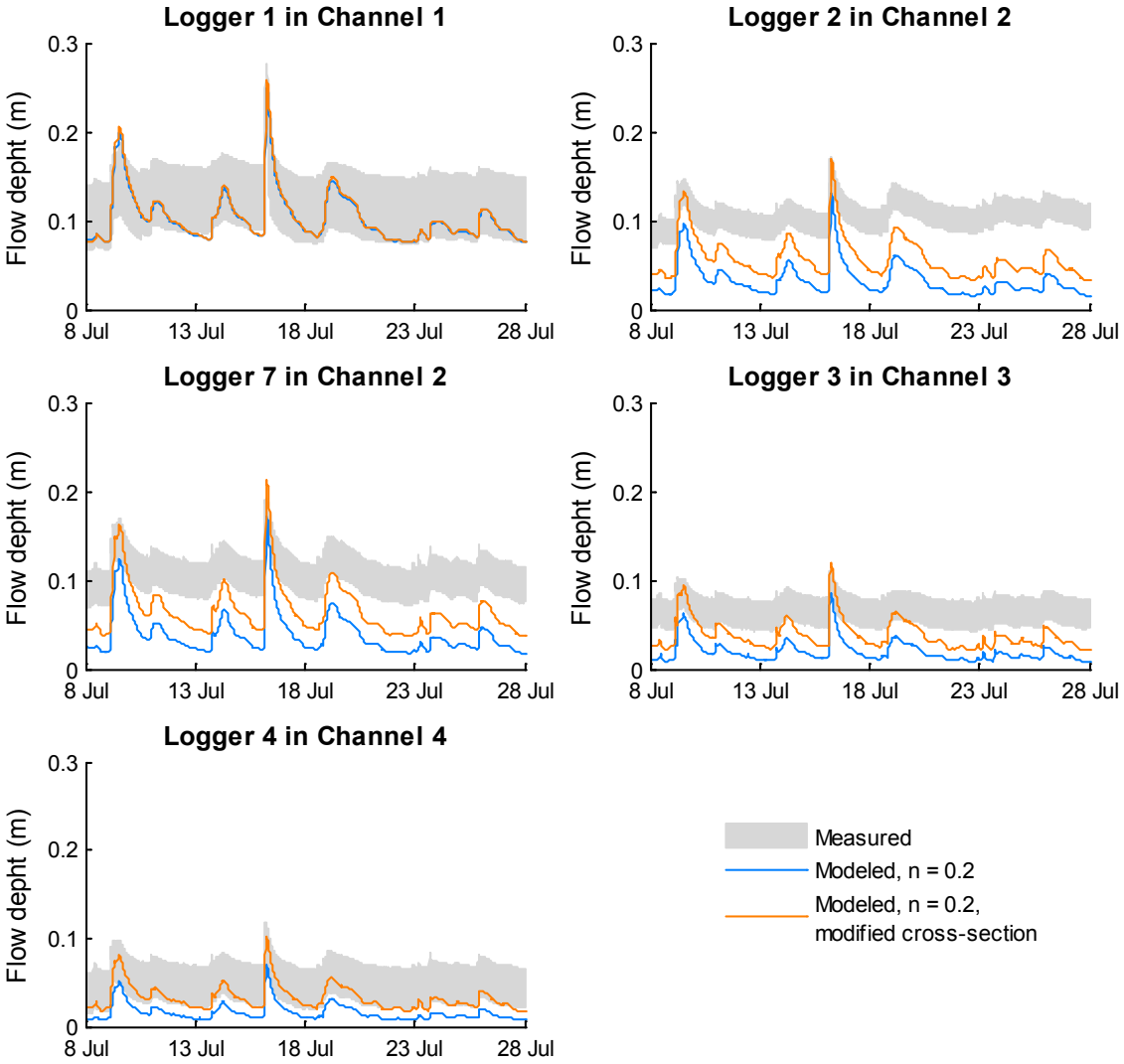

Figure 29 *Change in modeled flow depths in July 2012 in the Koivupuro ditch network when the bottom width of the cross-section of the ditches was modified from 0.35 m to 0.05 m (see Figure 8 for location of loggers*).

It can be questioned whether modeling flow in the northern ditches of the network is even worthwhile because even during the highest flow peak these upstream ditches re-

main almost dry (Figure 22b; Appendix 3). Besides, in terms of erosion and sediment transport the collecting ditches with higher discharge are the focus of interest (Joensuu et al. 1999). Leaving the northern ditches out of the hydraulic computation and replacing them by boundary conditions of incoming discharge at the beginning of ditches 2, 3 and 4 would simplify the model remarkably (Figure 30). We would end up with a network of 7 branches and no loops which would increase the computational efficiency. Also the discharge within the network would be more uniform and the concerning ditches in terms of stability would be left out of the simulation (e.g. the steepest ditch number 15).

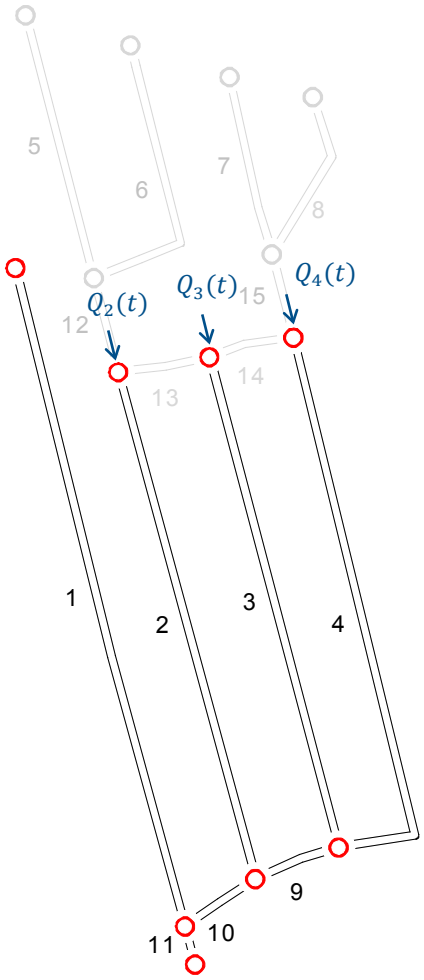

Figure 30 *The simplified Koivupuro ditch network with the upstream ditches of the catchment left out.*

The lag between the model input hydrograph and the modeled hydrograph at the outlet of the ditch network was about 45 minutes (Figure 31). It took thus 45 min for a flood wave to travel through the network. Increasing Manning's n would further increase the time lag but as we concluded earlier for this highest flow event $0.2 \leq n \leq 0.3$. However, lower flow peaks requiring higher Manning's n would have somewhat longer lag times. Figure 31 also shows the diffusion of the hydrograph and the lowering of the peak flow rate. The attenuation of the flood wave is partly due to the physical mechanisms associated with flood wave propagation (Cunge et al. 1980) but also caused by the way the flow enters the network along all channels, not just at the inlets of the network.

Figure 32 further shows that the chosen time step (Δt = 15 min) does not affect the lag time on the ditch network. Whether we applied Δt = 5 min or Δt = 30 min the form of the hydrograph remained almost the same.

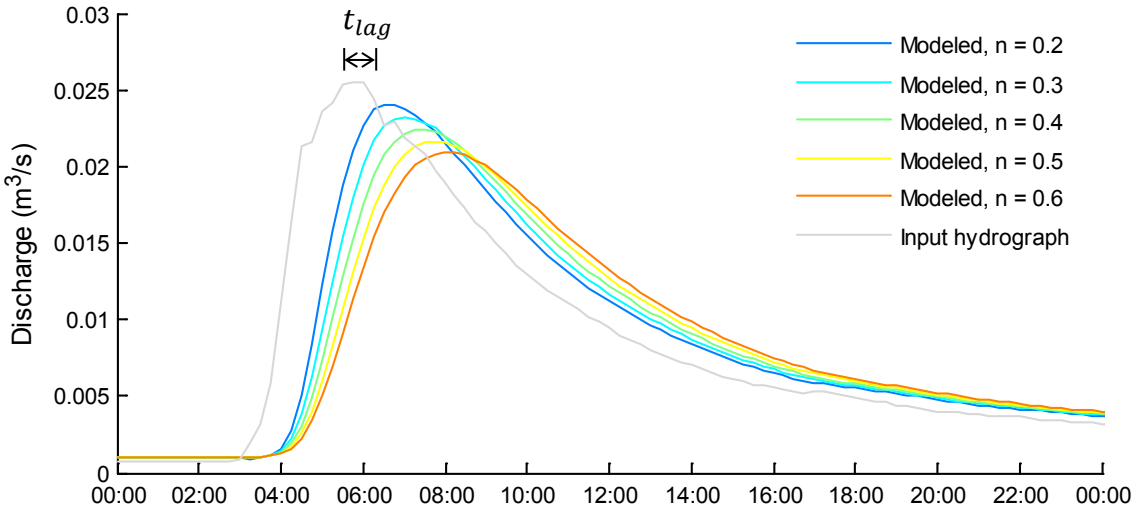

Figure 31 *Time lag (t_{lag}) between modeled discharge at the outlet of the Koivupuro ditch network with different Manning's n and the input hydrograph (i.e. the measured discharge at the catchment outlet) during the highest flow event on 16 July 2012.*

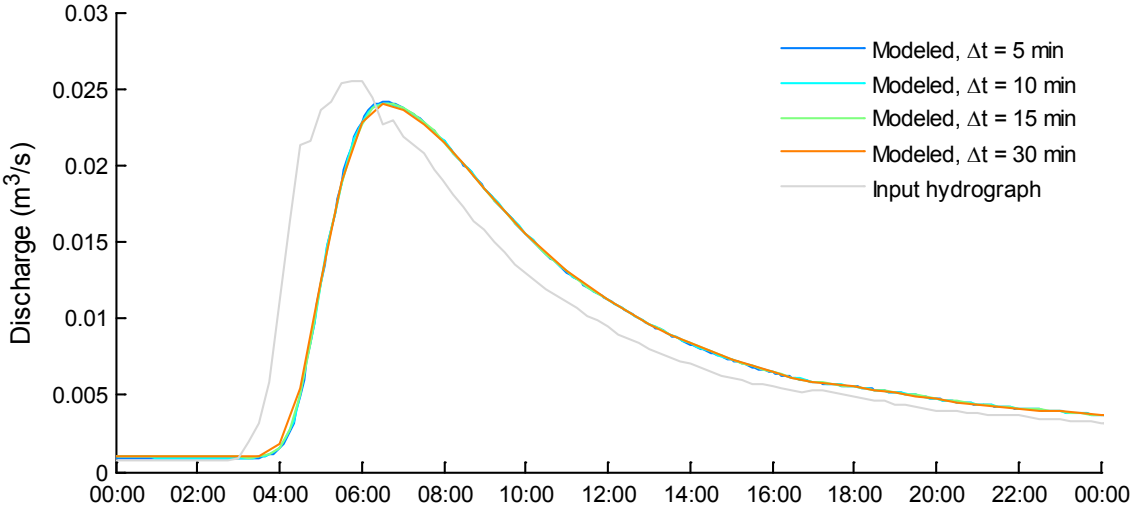

Figure 32 *Effect of the time step resolution on the modeled hydrograph at the outlet of the Koivupuro ditch network with n = 0.2 and the input hydrograph (i.e. the measured discharge at the catchment outlet) during the highest flow event on 16 July 2012.*

The time from the precipitation peak to the peak of the discharge at the outlet of the network was around 2 hours (Figure 33). The lag of 2 hours represents the time needed for the water input pulse to travel through the soil matrix (hydrology) and the ditch network (hydraulics). As Figure 31 illustrated the ditch network accounted for a lag of ca. 45 minutes which leads to the conclusion that the other half of the time elapsed from the precipitation event is due to hydrologic processes in the soil. Because of the small size of the catchment, the rather steep average slope (1 %) and the dense drainage network (ditch spacing 35 m) it can be argued whether lag times should be shorter. The equation proposed by Watt and Chow (1983) based on a large dataset of lag times of catchments of different size in North America would suggest a lag time of only 15

minutes for the Koivupuro catchment. The experimental equation presented by Watt and Chow (1983) does however take only the length and the average slope of the catchment into account. A catchment mainly covered by low conductive peat is likely to have a longer lag time than the one suggested by the expression of Watt and Chow (1983). Evaluating also the other flow events in July 2012 showed that the lag time of the Koivupuro catchment varied in the range of 1–2 hours. The fact that the precipitation was not measured at the study site Koivupuro but 3 km away at the Iso-Kauhea weather station may induce some uncertainty to the estimate of lag time.

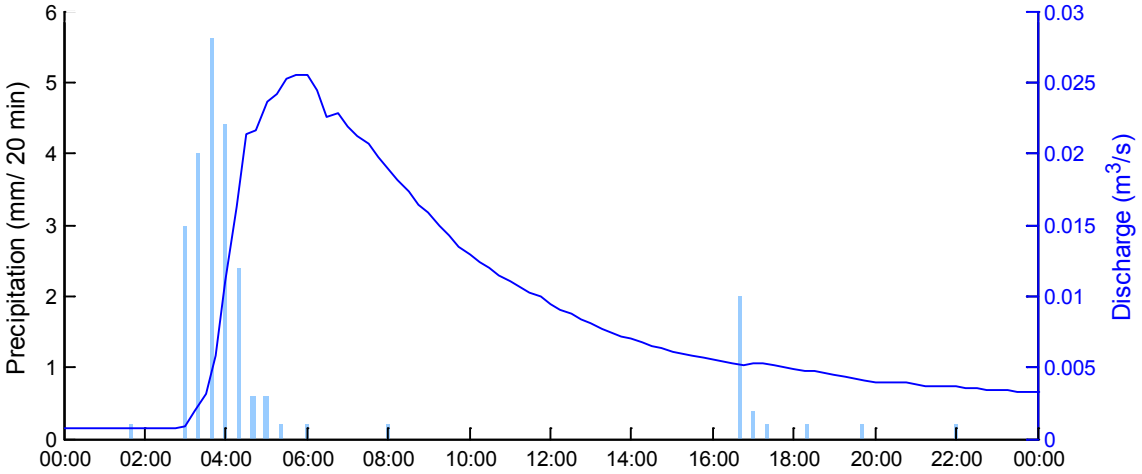

Figure 33 *Measured precipitation at the Iso-Kauhea weather station (3 km away) and measured discharge at the outlet of the Koivupuro ditch network during the highest flow event on 16 July 2012.*

5.3.3 FEMMA runoff as input of the hydraulic model

The catchment runoff produced by the hydrologic FEMMA model (see section 5.1) was experimented as model input for the same 20 days long period in July 2012. Figure 34 shows that using runoff simulated by FEMMA as the input to the hydraulic model results in a reasonable result compared to the modeled flow depth when the measured discharge was used as input. The same phenomenon of underestimation high flow peaks and overestimation of low flow peaks as observed in section 5.1 was present in the modeled flow depths too. Evidently the use of the measured discharge as input resulted in a better fit, but as measured runoff is not always available at reasonable resolution or at all, it is of interest to find out the performance of alternative model inputs. The resolution of the FEMMA runoff was 1 hour which was further interpolated to match the chosen time step (Δt = 15 min). Although the resolution was coarser than the resolution of the measured runoff it seemed to function rather well as input to the hydraulic model.

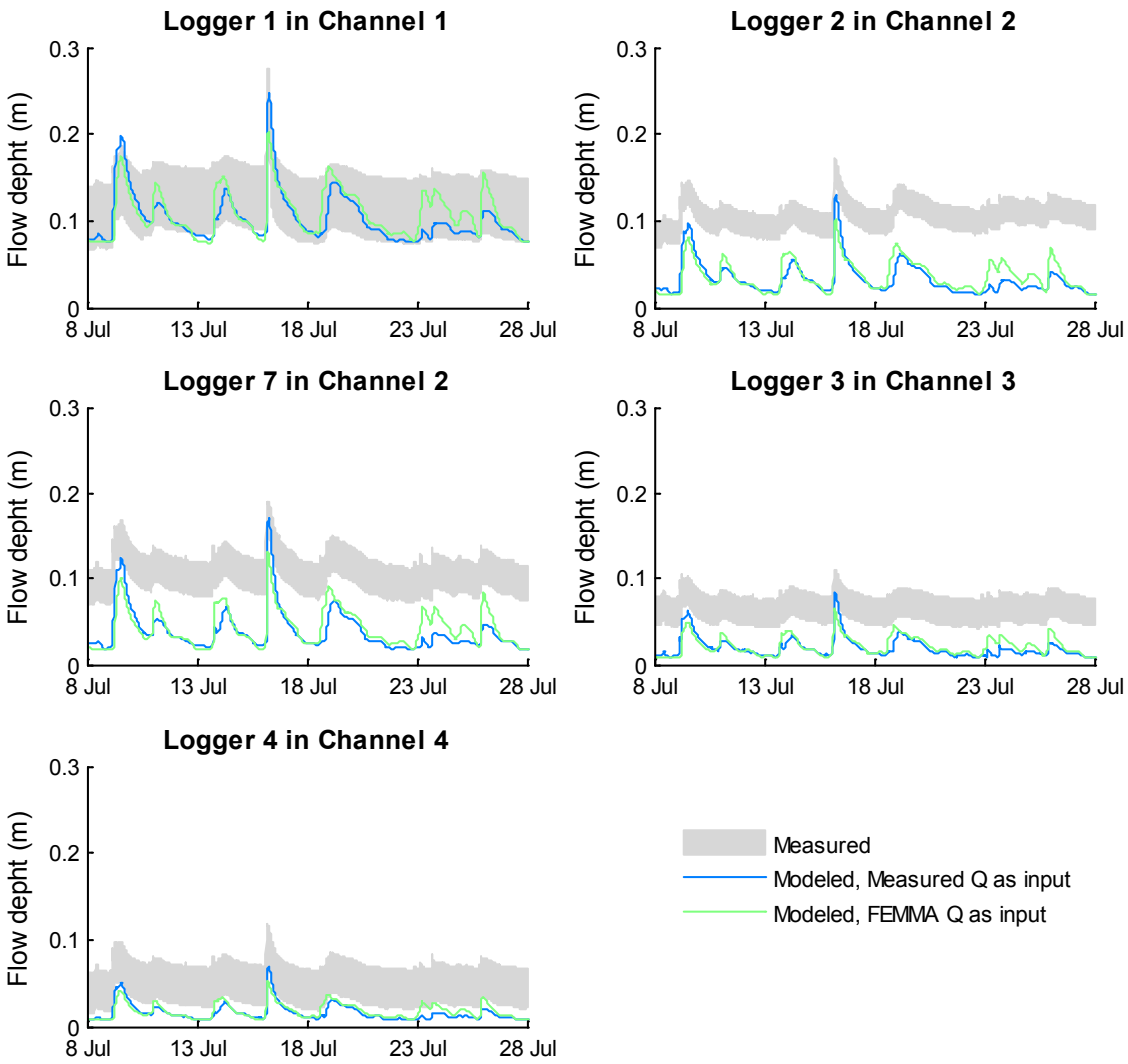

Figure 34 *Model output using the runoff simulated by the hydraulic FEMMA model as input compared to the model output using the measured runoff as input and to the actual measured flow depth error limits (see Figure 8 for location of loggers).*

5.4 Potential erosion

In regard to the uncertainties associated with the application of the model the simulation results provided the tools to assess the relative erosion risk in the different parts of the network rather than assessment of the actual erosion rate. According to model simulations during the highest flow event on 16 July 2012 flow velocity in the Koivupuro ditch network reached values up to 0.123 m/s (Figure 35). The highest values were reached in the steep parts of the four main ditches, especially in the steep southern end of the second ditch. The velocity profiles in Figure 35 were obtained with Manning's $n = 0.2$, which according to the discussion in the previous section may not be suitable for the entire ditch network since flow conditions vary a lot between the upstream and the downstream parts of the catchment. Figure 35 may thus be overestimating velocity in the upstream ditches and even in ditches 3 and 4, where flow rate was lower. According to the previously reported critical flow velocity values for peat (see Table 2) no erosion of the whole peat layer should occur. Erosion of the surface peat is likely to occur at least in the parts of the network presented in yellow to red in Figure 35, maybe even in the green to light blue areas (Kløve 1998; Marttila and Kløve 2008).

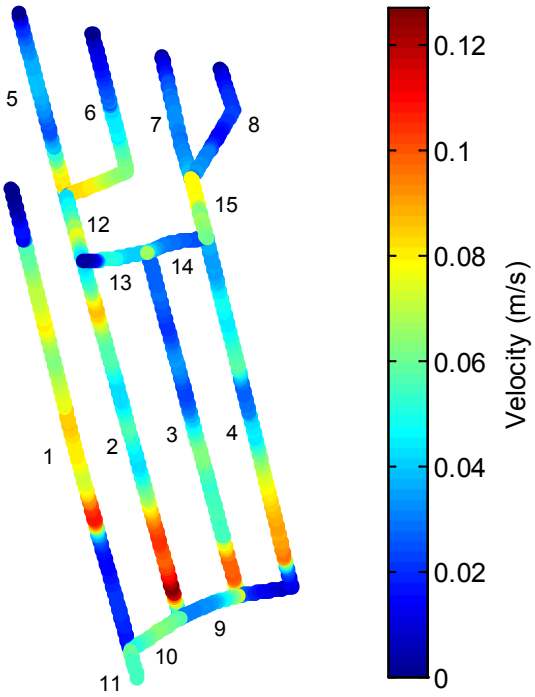

Figure 35 *Flow velocity in the Koivupuro ditch network (n = 0.2) during the peak flow rate on 16 July 2012.*

The simulated flow velocity was highly sensitive to the chosen Manning's coefficient (Figure 36). As we saw in section 5.3.2 in part of the ditches of the network Manning's n = 0.3 may be more suitable to represent flow resistance during the peak flow rate. Since the increase of Manning's n by 0.1 decreases the simulated flow velocity by about 20 % we should be very careful making conclusions of bed erosion in the network based on simulation with a single Manning's n for the whole network.

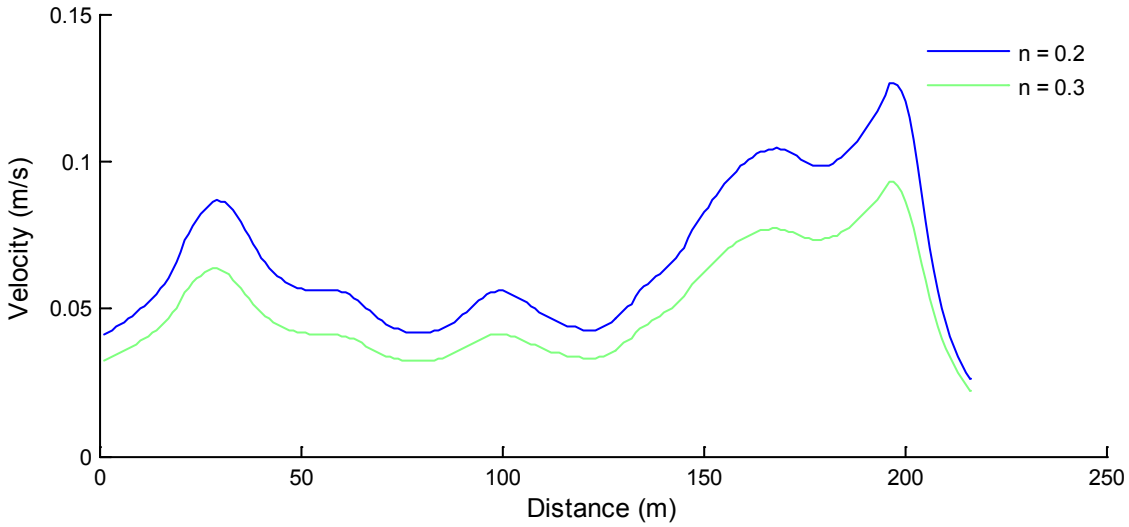

Figure 36 *Sensitivity of simulated flow velocity to Manning's coefficient in ditch number 2.*

As the Manning coefficient applied in the flow simulation did not represent only the roughness associated with the actual bed material, a different roughness coefficient (n = 0.021; Marttila and Kløve 2008) was used for the computation of bed shear stress.

Figure 37 shows bed shear stress in the Koivupuro ditch network that exceeds the critical shear stress of the whole peat layer (τ_{cr} = 0.059) reported by Marttila and Kløve (2008). Again, as in the evaluation of velocity, there was a distinct difference in the results depending on whether n = 0.2 or n = 0.3 was applied in the flow simulation. Because of the varying flow conditions in the network the results of Figure 37a are only applicable for southern part of the network maybe even only for the downstream of ditches 1 and 2. For the rest of the network Figure 37b suggest that no erosion of the whole peat layer would occur. The parts of the network with the highest erosion risk are thus in the steepest parts of the ditches 1 and 2, especially in the steep end of ditch 2 where most of the flow accumulates. Nevertheless, it should be noted that while the critical shear stress of the whole peat layer was not exceeded in the majority of the ditches during summer peak flows in 2012, particles of the loose surface layer might get detached more easily. Especially during the first years after ditch maintenance this loose surface layer is probable to increase the total sediment load from the catchment. Also the peat type, rate of decomposition and density may affect the critical shear stress of the bed material (Marttila and Kløve 2008).

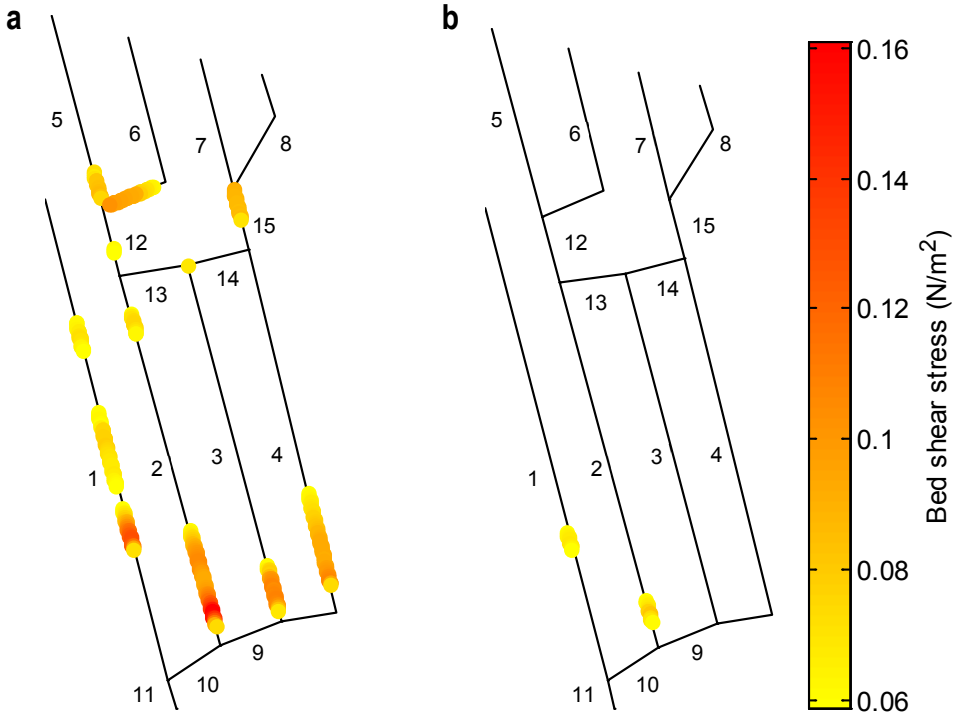

Figure 37 *Bed shear stress in the Koivupuro ditch network during the highest flow peak on 16 July 2012 when Manning's n = 0.2 (a) and Manning's n = 0.3 (b). Only the values higher than the critical shear stress τ_{cr} = 0.059 (Marttila and Kløve 2008) are shown.*

The evaluation of both flow velocity and bed shear stress signaled that the erosion risk was the highest in the downstream part of the four main ditches (ditches 1, 2, 3 and 4). In the Koivupuro ditch network the collecting ditch in the south of the catchment did not seem to have a tendency for erosion probably because of the damming effect which prevented flow of high velocity. These results strengthen the motives to simulate flow in a simpler version of the network where the upstream ditches are left out of the computation (Figure 30). All in all, erosion seemed to have a rather minor role during sum-

mer peak discharge in the studied ditch network. This was in accordance with visual observations made at the Koivupuro nested catchment which indicated a lot of siltation in the ditches. However, it can be expected that during spring snow melt when runoff may be even twice as high, more remarkable erosion would occur (Marttila and Kløve 2010).

6 Conclusions

The main objective of this study was to build a hydraulic unsteady flow model that would meet the needs of flow simulation in a drainage network on a forested peatland site. The suspended solid (SS) load following ditch network maintenance on drained peatlands causes one of the largest strains on the water system by forestry. Understanding the hydraulic processes in newly maintained ditch networks on drained peatland sites is necessary in the assessment of spatial distribution of the SS load generation from peatlands and of great importance in water protection work.

The hydraulic model was built for a network of channels where junction-points could be both diverging and converging. Neither the total number of branches nor the number of branches meeting at a junction-point were restricted in the model. The Saint-Venant equations were applied to simulate unsteady flow in the channels of the network. The governing equations were solved numerically using the four-point implicit Preissmann scheme and the Newton-Raphson iterative method. The junction-point flow depth prediction and correction algorithm proposed by Zhu et al. (2011) was applied to link the branches of the network together and incorporate backwater effects. The algorithm consists of prediction of flow depth at the junctions and their correction based on the characteristic method at each iteration round until convergence is reached. To accurately represent the accumulation of flow in the drainage network lateral inflow was incorporated in the hydraulic model. The whole algorithm was programmed using the numeric computing environment MATLAB by MathWorks.

The model was applied to a newly maintained ditch network on a drained peatland catchment Koivupuro in Eastern Finland. The catchment was ca. 5.2 ha in size and the total length of the ditches in the network was 1.6 km with 15 branches and 8 junctions. The measured discharge at the outlet of the ditch network was used as the model input such that it was distributed along the ditches based on the topography of the catchment area. All the runoff was assumed to be generated on the catchment area thus no flow boundaries were set at the upstream ends of the network. The discharge measurement weir at the outlet of the network defined a relation between discharge and flow depth as the downstream boundary. The model was applied to a 20 day long period in July 2012 with discharge varying between 0.0005…0.025 m^3/s.

Flow simulation in small ditches with mostly very low flow rate introduced its challenges. First of all, we were forced to use a short distance step of 1 m in the simulation to avoid unrealistic results. $\Delta x = 1$ m led up to 279 computation nodes in the longest ditch. This along with the rather complex characteristics of the network resulted in long running times. Secondly, the Manning's roughness coefficient reported in literature did not seem applicable to the flow conditions of the Koivupuro ditch network. Earlier reports from Finnish drained peatland sites have applied Manning's roughness coefficients in the range of 0.02–0.04 (Marttila and Kløve 2008; Tuukkanen 2010; Lappalainen et al. 2010).

Evaluation based on the measured flow depths at Koivupuro and model simulations showed that Manning's coefficient should be higher than 0.2. The magnitude of Manning's coefficient depended on the flow conditions. Evidently no one single Manning's coefficient could be applied for the full range of flow conditions or even for the whole network as differences in discharge were large even within the network at the same time step. A clear relationship was observed between the turbulence of flow (Reynolds number) and Manning's flow resistance coefficient. The relationship was in good accordance with the results reported by Hosia (1980) for small earth channels in Finland. The variability of flow resistance introduced an inevitable challenge to flow computation over a longer time period in a network of such small scale. It can be argued whether flow simulation in the whole network is even worthwhile. As we assumed all the runoff was generated within the catchment the flow rate in the upstream ditches of the network remained very low throughout the simulation period. A scenario including only the main ditches of the network in the flow simulation model could be a noteworthy future prospect.

Model simulations during low flow conditions suggested that flow resistance should be increased to $n \geq 3$. In regard to literature this seemed rather extreme and raised the question whether there were other sources of error. The measured flow depths were subject to uncertainty. Although the fluctuation of water level in the ditches was undoubtedly well captured by the loggers the absolute level of the water in the ditches was uncertain. Firstly, the loggers were not leveled in 2012 and secondly the location of the bottom of the ditches was difficult to determine because of the high porosity of the bed material peat. Another probable source of error to the modeled flow depth profiles could be the assumed constant cross-section of the ditches. In the model the cross-section had a horizontal bottom width of 0.35 m, but in reality flow is likely to have shaped the bottom of the ditches forming a narrower flow path for low flow conditions.

Based on the precipitation and the discharge measurements the lag time of the Koivupuro catchment was 1–2 hours. This was rather long compared to values reported in the literature (e.g. Watt and Chow 1983). The hydraulic modeling suggested that about 45 minutes would be due to the flow traveling through the ditch network. The estimate is however highly dependent of the applied flow resistance and may thus be different for flow events of different magnitude.

The potential erosion in the Koivupuro ditch network was evaluated by means of bed shear stress. As flow resistance was expected to vary within the network it was difficult to draw conclusions of potential erosion in absolute terms. However, in relative terms it seemed that the most erosion sensitive areas were in the southern end of the first and second ditch where most of the flow accumulates and which have steep reaches. In accordance with previous studies on drained peatlands (e.g. Marttila and Kløve 2008), it can be expected that only highest peak flows have a role in SS generation in the Koivupuro ditch network.

References

Aho, M. and Kantola, K. 1985. Sedimentation of suspended solids in peat harvesting runoff waters (in Finnish). Governmental Research Center, Espoo, Finland.

Asano, Y. and Uchida, T. 2011. Measuring flow and Manning's roughness coefficient at small mountain stream. American Geophysical Union, Fall Meeting 2011, abstract #EP21C-0712.

Chanson, H. 2004. *Hydraulics of open channel flow*. Butterworth-Heinemann. 650 pp.

Chow, V. T. 1959. *Open-Channel Hydraulics*. New York: McGraw-Hill. 680 pp.

Cunge, J. A., Holly, F. M. and Verwey, A. 1980. *Practical aspects of computational river hydraulics*. Pitman, Boston. 420 pp.

Finnish Meteorological Intitute. 2012. Joulukuun ilmastokatsuas, Ilmastokatsaus arkisto. Webpublication. Available at: http://ilmatieteenlaitos.fi/c/document_library/get_file?uuid=43a0679b-ee9a-464c-9680-e49bf2c82ff8&groupId=30106. Cited 21.8.2013.

Finnish Statictical Yearbook of Forestry 2012. Finnish Forest research Institute. Vantaa.

Fread, D. L. 1973a. Technique for implicit dynamic routing in rivers with tributaries. Water Resources Research, 9(4): 918–926.

Fread, D. L. 1973b. Effects of time step size in implicit dynamic routing. Journal of the American Water Resources Association, 9(2): 338–351.

Fread, D.L. and Lewis, J.M. 1993. Selection of Δx and Δt computational steps for four-point implicit nonlinear dynamic routing models. In: Shen, H. W., Su, S. T. and Wen, F. (eds.). *Hydraulic engineering 1993.* Conference proceedings, San Francisco, CA. July 25–30, 1993. American Society of Civil Engineers. New York. pp. 1569–1573.

French, R. H. 1986. *Open-channel Hydraulics.* McGraw-Hill, New York. 705 pp.

Graf, W. H. 1984. *Hydraulics of sediment transport*. McGraw-Hill Series in Water Resources and Environmental Engineering, Colorado. 513 pp.

Heikkinen, M. 2004. Design of peak runoff control method for water protection on peat harvesting areas (in Finnish). Master's thesis, University of Oulu. Department of Process and Environmental Engineering. Oulu.

Hosia, L. 1980. Pienten uomien virtausvastuskerroin. Vesihallituksen tiedotus 199. Vesihallitus, Helsinki. 119 pp.

Hökkä, H., Koivusalo, H., Ahti., E., Nieminen, M., Laine, J., Saarinen, M., Laurén, A., Alm, J., Nikinmaa, E., Kløve, B. and Marttila, H. 2008. Effects of tree stand transpiration and interception on site water balance in drained peatlands: experimental design and measurements. In: Farrell, C. & Feehan, J. (eds.). *After wise use - The future of*

peatlands. Proceedings of the 13th international peat congress, Tullamore, Ireland. June 8–13, 2008. International Peat Society. pp. 169–171.

Islam, A., Raghuwanshi, N. S., Singh, R. and Sen, D. J. (2005). Comparison of gradually varied flow computation algorithms for open-channel network. Journal Irrigation and Drainage Engineering, 131(5): 457–465.

Jenson, S. K. and Domingue, J. O. 1988. Extracting topographic structure from digital elevation data for geographic information system analysis. Photogrammetric Engineering and Remote Sensing, 54(11): 1593–1600.

Joensuu, S., Ahti, E. and Vuollekoski, M. 1999. The effects of peatland forest ditch maintenance on suspended solids in runoff. Boreal Environment Research, 4(4): 343–355.

Järvelä, J. 1998. Luonnonmukainen vesirakennus: periaatteet ja hydrauliset näkökohdat virtavesien ennallistamisessa ja uudisrakentamisessa, (Environmental river engineering and restoration: guiding principles and hydraulic performance). Espoo: Helsinki University of Technology. 129 p. Helsinki University of Technology Water Resources Publications, 1. TKK-VTR-1. ISBN: 951-22-4296-6, ISSN: 1456-2596.

Järvelä, J. and Helmiö, T. 2004. Hydraulic Considerations in Restoring Boreal Streams. Nordic Hydrology [Electronic Journal], 35(3): 223–235. [Cited 21 October 2013]. Available at: http://www.iwaponline.com/nh/035/nh0350223.htm.

Kellomäki S. 1999. Calculation of foliage mass and foliage area. In: Laurila, T. and Lindfors, V. (eds.), Biogenic VOC emissions and photochemistry in the boreal regions of Europe, Air Pollution Research Report 70, Commission of the European Communities, Luxembourg, pp. 113–125.

Kløve, B. 1998. Erosion and sediment delivery from peat mines. Soil and Tillage Research, 45(1): 199–216.

Koivusalo, H., Kokkonen, T., Laurén, A., Ahtiainen, M., Karvonen, T., Mannerkoski, H., Penttinen, S., Seuna, P., Starr, M. and Finér, L. 2006. Parameterisation and application of a hillslope hydrological model to assess impacts of a forest clear-cutting on runoff generation. Environmental Modelling & Software, 21(9): 1324–1339.

Koivusalo, H., Laurén, A. and Kokkonen, T. 2009. FEMMA – forest hydrological and water quality model: Documentation of hydrological submodels. Unpublished draft.

Koivusalo, H., Starr, M., Laurén, A. and Finér, L. 2007. Päätehakkuun ja maanmuokkauksen vaikutus veden kiertoon ja ravinnekuormitukseen. Metsätieteen aikakauskirja 3/2007, 296–301.

Koivusalo, H., Hökkä, H., Laurén, A., Nikinmaa, E., Laine, J. and Ahti, E. 2008a. Splitting the water balance of drained peatland forests into hydrological components. In:

Farrell, C. & Feehan, J. (eds.). *After wise use – The future of peatlands*. Proceedings of the 13th international peat congress, Tullamore, Ireland. June 8–13, 2008. International Peat Society. pp. 485–487.

Koivusalo, H., Lappalainen, M., Ahti, E., Laurén, A., Nieminen, M., Leinonen, A., Joensuu, S. and Nevalainen, R. 2008b. Miten metsätalous vaikuttaa kiintoaineen kulkeutumiseen? Vesitalous 6/2008, 15–18.

Lappalainen, M. 2008. Transport of sediment from peatland forests after ditch network maintenance. Master's thesis. Helsinki University of Technology, Department of Civil and Environmental Engineering. Espoo. 86 pp.

Lappalainen,M., Koivusalo, H., Karvonen, T. and Laurén, A. 2010. Sediment transport from a peatland forest after ditch network maintenance: a modeling approach. Boreal Environment research, 15(6): 595–612.

Marttila, H. and Kløve, B. 2008. Erosion and delivery of deposited peat sediment. Water Resources Research, 44(6): W06406.

Marttila, H. and Kløve, B. 2010. Dynamics of erosion and suspended sediment transport from drainedpeatland forestry. Journal of Hydrology 388 (3–4): 414–425.

McAnally, W. and Mehta, A. 2000. Aggregation Rate of Fine Sediment. Journal of Hydraulic Engineering, 126(12): 883–892.

Naidu, B. J., Bhallamudi, S. M. and Narasimhan, S. 1997 "GVF computation in tree-type networks. Journal of Hydraulic Engineering, 123(8): 700–708.

Nguyen, Q. K. and Kawano, H. 1995. Simultaneous solution for flood routing in channel networks. Journal of Hydraulic Engineering, 121(10): 744–750.

Niemi, T. 2010. Development of a hydraulic model and its application to a small urban stream. Master's thesis. Aalto University, School of science and technology, Faculty of Engineering and Architecture. Espoo. 74 pp.

Parchure, T. M. and Mehta, A. J. 1985. Erosion of soft cohesive sediment deposits. Journal of Hydraulic Engineering, 111(10): 1308–1326.

Peltomaa, R. 2007. Drainage of forests in Finland. Irrigation and Drainage, 56(1): 151–159.

Pomeroy, J. W., Gray, D. M., Hedstrom, N. R. and Janowicz, J. R. 2002. Physically based estimation of seasonal snow accumulation in the boreal forest. In: Proceedings of the Eastern Snow Conference, Stowe, Vermont, USA, pp. 93–108.

Päivänen, J. 2007. *Suot ja suometsät – järkevän käytön perusteet*. Helsinki: Metsäkustannus Oy. 368 pp.

Repola, J., Ojansuu, R. and Kukkola, M. 2007. Biomass functions for Scots pine, Norway spruce and birch in Finland. Working Papers of the Finnish Forest Research Institute 53. 28 pp.

Saari, S. 1955. Hankauskertoimen arvosta pienissä vesiväylissä. Master's thesis. Helsinki University of Technology. Espoo. 105 pp.

Sarkkola, S., Nieminen, M., Ahti, E., Hökkä, H., Koivusalo, H., Päivänen, J. and Laine, J. 2010. Role of tree stand evapotranspiration in maintaining satisfactory drainage conditions in drained peatlands. Canadian Journal of Forest Research, 40(8): 1485–1496.

Sarkkola, S., Hökkä, H., Nieminen, M., Koivusalo, H., Laurén, A., Ahti, E., Launiainen, S., Marttila, H. and Laine, J. 2012. Can tree stand water use compensate for maintenance of ditch networks in peatlands? Implications from water balance measurements. In: Magnusson, T. (eds.). Abstracts of the 14th International Peat Congress. Stockholm, 3.–8.6. 2012. Abstract No. 53.

Scholz, M. and Trepel, M. 2004. Hydraulic characteristics of groundwater-fed open ditches in a peatland. Ecological Engineering, 23(1): 29–45.

Seibert, J. and McGlynn, B. L. 2007. A new triangular multiple flow direction algorithm for computing upslope areas from gridded digital elevation models. Water Resources Research, 43(4): W04501.

Sen, D. J. and Garg, N. K. 2002. Efficient algorithm for gradually varied flows in channel networks. Journal Irrigation and Drainage Engineering, 128(6): 351–357.

Seuna, P. and Vehviläinen, B. 1986. Eroosio ja kiintoaineen kulkeutuminen. In: Mustonen, S. (eds.) Sovellettu hydrologia. Vesiyhdistys r.y. Helsinki. pp. 226–290.

Szymkiewicz, R. 2010. *Numerical modeling in open channel hydraulics*. Springer, Dordrecht. 419 pp.

Turunen, M. 2011. Pellon vesitaseen ja salaojitusmenetelmien toimivuuden analyysi (Abstract: Analysis of the water balance and subsurface drainage methods in an agricultural field). Master's thesis. Aalto University, School of engineering, Department of Civil and Environmental Engineering. Espoo. 125 pp.

Tuukkanen, T. 2010. RiverLifeGIS -paikkatietotyökalun soveltuvuus turvemetsätalouden ojaeroosioriskin arviointiin (Abstract: Suitability of RiverLifeGIS - geographical information tool for ditch erosion risk assessment in peatland forestry). Master's thesis. University of Oulu, Department of Process and Environmental Engineering. Oulu. 144 pp.

van Genuchten, M. T. 1980. A closed-form equation for predicting the hydraulic conductivity of unsaturated soils. Soil Science Society of America Journal, 44(5): 892–898.

van Rijn, L. C. 1984. Sediment transport, Part I: Bed load transport. Journal of Hydraulic Engineering 110(10): 1431–1456.

Vanoni, V. A. 1984. Fifty years of sedimentation. Journal of Hydraulic Engineering, 110(8): 1021–1057.

Venutelli, M. 2002. Stability and Accuracy of Weighted Four-Point Implicit Finite Difference Schemes for Open Channel Flow. Journal of Hydraulic Engineering, 128(3): 281–288.

Walczak, R., Rovdan, E. and Witkowska-Walczak, B. 2002. Water retention characteristics of peat and sand mixtures. International Agrophysics, 16(2): 161–165.

Watt, W. E. and Chow, K. A. 1985. A general expression for basin lag time. Canadian Journal of Civil Engineering, 12(2): 294–300.

Zhu, D., Chen, Y., Wang, Z. and Liu, Z. 2011. Simple, robust, and efficient algorithm for gradually varied subcritical flow simulation in general channel networks. Journal of Hydraulic Engineering, 137(7): 766–774.

List of appendices

Appendix 1. Partial derivatives of the discretized Saint-Venant equations

Steady-state

Continuity

$$\frac{\partial F_1}{\partial Q_i} = -\frac{1}{\Delta x} \qquad \frac{\partial F_1}{\partial h_i} = 0 \qquad \frac{\partial F_1}{\partial Q_{i+1}} = \frac{1}{\Delta x} \qquad \frac{\partial F_1}{\partial h_{i+1}} = 0$$

Momentum

$$\frac{\partial F_2}{\partial Q_i} = -\frac{2Q_i}{\Delta x A_i} + \frac{gn^2|Q_i|}{A_i R_i^{4/3}}$$

$$\frac{\partial F_2}{\partial h_i} = \frac{T_i}{\Delta x}\left(\frac{Q_i}{A_i}\right)^2 + \frac{g}{2\Delta x}[T_i(h_{i+1} - h_i) - A_i - A_{i+1}] - \frac{gn^2 Q_i|Q_i|}{2A_i R_i^{4/3}}\left(\frac{T_i}{A_i} + \frac{4\frac{\partial R_i}{\partial h_i}}{3R_i}\right) - \frac{gT_i S_{0,i+1/2}}{2}$$

$$\frac{\partial F_2}{\partial Q_{i+1}} = \frac{2Q_{i+1}}{\Delta x A_{i+1}} + \frac{gn^2|Q_{i+1}|}{A_{i+1} R_{i+1}^{4/3}}$$

$$\frac{\partial F_2}{\partial h_{i+1}} = -\frac{T_{i+1}}{\Delta x}\left(\frac{Q_{i+1}}{A_{i+1}}\right)^2 + \frac{g}{2\Delta x}[T_{i+1}(h_{i+1} - h_i) + A_i + A_{i+1}]$$
$$- \frac{gn^2 Q_{i+1}|Q_{i+1}|}{2A_{i+1} R_{i+1}^{4/3}}\left(\frac{T_{i+1}}{A_{i+1}} + \frac{4\frac{\partial R_{i+1}}{\partial h_{i+1}}}{3R_{i+1}}\right) - \frac{gT_{i+1}S_{0,i+1/2}}{2}$$

Unsteady flow

Continuity

$$\frac{\partial F_1}{\partial Q_i^{k+1}} = -\frac{\alpha}{\Delta x} \qquad \frac{\partial F_1}{\partial h_i^{k+1}} = \frac{T_i^{k+1}}{2\Delta t} \qquad \frac{\partial F_1}{\partial Q_{i+1}^{k+1}} = \frac{\alpha}{\Delta x} \qquad \frac{\partial F_1}{\partial h_{i+1}^{k+1}} = \frac{T_{i+1}^{k+1}}{2\Delta t}$$

Momentum

$$\frac{\partial F_2}{\partial Q_i^{k+1}} = \frac{1}{2\Delta x} - \frac{2\alpha Q_i^{k+1}}{\Delta x A_i^{k+1}} + \frac{gn^2\left|Q_i^{k+1}\right|}{A_i^{k+1}(R_i^{k+1})^{4/3}}$$

$$\frac{\partial F_2}{\partial h_i^{k+1}} = \frac{\alpha T_i^{k+1}}{\Delta x}\left(\frac{Q_i^{k+1}}{A_i^{k+1}}\right)^2 + \frac{g\alpha}{2\Delta x}\left(T_i^{k+1}h^* - A^{**}\right) - \frac{gn^2\alpha Q_i^{k+1}\left|Q_i^{k+1}\right|}{2A_i^{k+1}(R_i^{k+1})^{4/3}}\left(\frac{T_i^{k+1}}{A_i^{k+1}} + \frac{4\frac{\partial R_i^{k+1}}{\partial h_i^{k+1}}}{3R_i^{k+1}}\right)$$
$$- \frac{g\alpha T_i^{k+1}S_{0,i+1/2}}{2}$$

$$\frac{\partial F_2}{\partial Q_{i+1}^{k+1}} = \frac{1}{2\Delta x} + \frac{2\alpha Q_{i+1}^{k+1}}{\Delta x A_{i+1}^{k+1}} + \frac{gn^2\left|Q_{i+1}^{k+1}\right|}{A_{i+1}^{k+1}(R_{i+1}^{k+1})^{4/3}}$$

$$\frac{\partial F_2}{\partial h_{i+1}^{k+1}} = \frac{\alpha T_{i+1}^{k+1}}{\Delta x}\left(\frac{Q_{i+1}^{k+1}}{A_{i+1}^{k+1}}\right)^2 + \frac{g\alpha}{2\Delta x}\left(T_{i+1}^{k+1}h^* - A^{**}\right) - \frac{gn^2\alpha Q_{i+1}^{k+1}\left|Q_{i+1}^{k+1}\right|}{2A_{i+1}^{k+1}(R_{i+1}^{k+1})^{4/3}}\left(\frac{T_{i+1}^{k+1}}{A_i^{k+1}} + \frac{4\frac{\partial R_{i+1}^{k+1}}{\partial h_{i+1}^{k+1}}}{3R_{i+1}^{k+1}}\right)$$
$$- \frac{g\alpha T_{i+1}^{k+1}S_{0,i+1/2}}{2}$$

where $h^* = \alpha\left(h_{i+1}^{k+1} - h_i^{k+1}\right) + (1-\alpha)\left(h_{i+1}^{k} - h_i^{k}\right), A^{**} = \alpha(A_{i+1}^{k+1} + A_i^{k+1}) + (1-\alpha)(A_{i+1}^{k} + A_i^{k})$

Appendix 2. Detailed flowchart of the programmed unsteady flow simulation algorithm

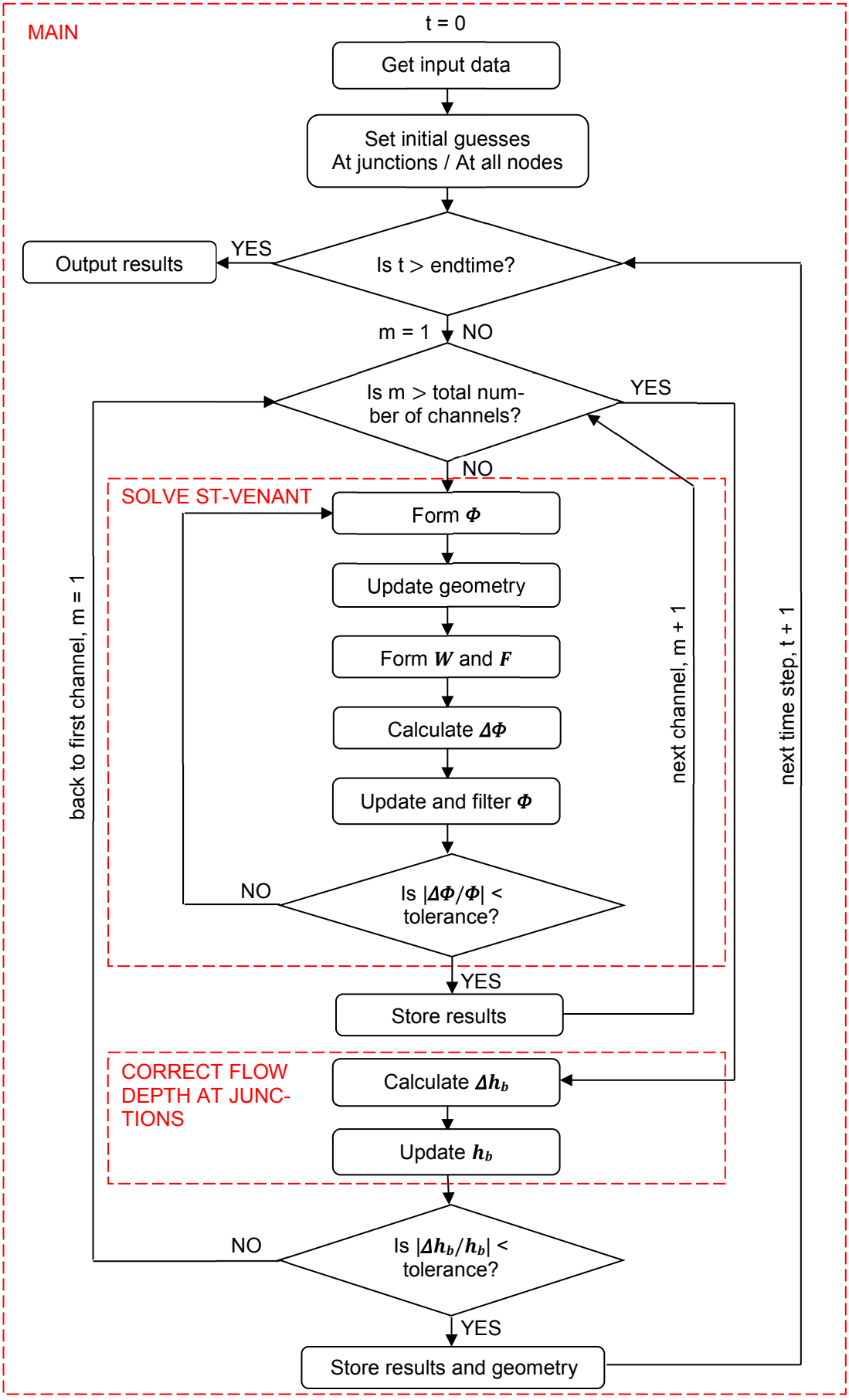

Appendix 3. Water level in channels of the Koivupuro ditch network during high flow peak on 16 July 2012